frontiers | Frontiers in Earth Science

TYPE Original Research
PUBLISHED 03 October 2023
DOI 10.3389/feart.2023.1197568

OPEN ACCESS

EDITED BY
Varsha Srivastava,
University of Oulu, Finland

REVIEWED BY
Roberto Moretti,
UMR7154 Institut de Physique du Globe de Paris (IPGP), France
Takeshi Ohba,
Tokai University, Japan

*CORRESPONDENCE
Claudio Inguaggiato,
inguaggiato@cicese.mx

RECEIVED 31 March 2023
ACCEPTED 11 September 2023
PUBLISHED 03 October 2023

CITATION
Pappaterra S, Inguaggiato C, Rouwet D, Levresse G, Peiffer L, Apollaro C, Mora-Amador R, Ramírez-Umaña C, González G, Schiavo B, Kretzschmar TG and Brusca L (2023), Fluid-mineral dynamics at the Rincón de la Vieja volcano—hydrothermal system (Costa Rica) inferred by the study of major, minor and rare earth elements in the hyperacid crater lake.
Front. Earth Sci. 11:1197568.
doi: 10.3389/feart.2023.1197568

Fluid-mineral dynamics at the Rincón de la Vieja volcano—hydrothermal system (Costa Rica) inferred by the study of major, minor and rare earth elements in the hyperacid crater lake

Sabrina Pappaterra[1], Claudio Inguaggiato[2,3]*, Dmitri Rouwet[3], Gilles Levresse[4], Loic Peiffer[2,5], Carmine Apollaro[6], Raúl Mora-Amador[7], Carlos Ramírez-Umaña[8], Gino González[3,9,10], Benedetto Schiavo[11], Thomas Gunter Kretzschmar[2] and Lorenzo Brusca[12]

[1]Posgrado en Ciencias de la Tierra, Centro de Investigación Científica y de Educación Superior de Ensenada, Baja California (CICESE), Carretera Ensenada-Tijuana, Ensenada, Mexico, [2]Departamento de Geología, Centro de Investigación Científica y de Educación Superior de Ensenada, Baja California (CICESE), Carretera Ensenada-Tijuana, Ensenada, Mexico, [3]Istituto Nazionale di Geofisica e Vulcanologia, Sezione di Bologna, Bologna, Italy, [4]Centro de Geociencias, Querétaro, Mexico, [5]Unidad La Paz (ULP), Centro de Investigación Científica y Educación Superior de Ensenada, Baja California (CICESE), La Paz, Mexico, [6]Dipartimento di Biologia, Ecologia e Scienze della Terra, Università della Calabria, Arcavacata di Rende, Cosenza, Italy, [7]Centro de Investigaciones en Ciencias Geológicas, Universidad de Costa Rica, San José, Costa Rica, [8]Servicio Geológico Ambiental de Costa Rica (SeGeoAm), San José, Costa Rica, [9]Dipartimento di Scienze della Terra e Geoambientali, Università degli studi di Bari Aldo Moro, Bari, Italy, [10]Volcanes sin Fronteras, San José, Costa Rica, [11]Instituto de Geofísica, Universidad Nacional Autónoma de México, Mexico City, Mexico, [12]Istituto Nazionale di Geofisica e Vulcanologia, Sezione di Palermo, Palermo, Italy

Volcanic lakes are complex natural systems and their chemical composition is related to a myriad of processes. The chemical composition of major, minor, Rare Earth Elements (REE) and physico-chemical parameters at the hyperacid crater lake of Rincón de la Vieja volcano (Costa Rica) are here investigated during February 2013–August 2014. The study of the lake chemical composition allows to identify the main geochemical processes occurring in the lake and to track the changes in the volcanic activity, both important for active volcanoes monitoring. The total REE concentration (∑REE) dissolved in the crater lake varies from 2.7 to 3.6 mg kg^{-1} during the period of observation. REE in the water lake samples normalized to the average volcanic local rock ($REE_{N\text{-local rock}}$) are depleted in light REE (LREE). On the contrary $REE_{N\text{-local rock}}$ in the solids precipitated (mainly gypsum/anhydrite), from lake water samples in laboratory at 22°C, are enriched in LREE. The low variability of $(La/Pr)_{N\text{-local rock}}$ and $(LREE/HREE)_{N\text{-local rock}}$ ratios (0.92–1.07 and 0.66–0.81, respectively) in crater lake waters is consistent with the low phreatic activity (less than 10 phreatic eruptions in 2 years) observed during the period of observation. This period of low activity precedes the unrest started in 2015, thus, it could be considered as a pre-unrest, characterized by infrequent phreatic eruptions. No clear changes in the REE chemistry are associated with the phreatic eruption occurred at mid-2013. The results obtained investigating water-rock interaction processes at the

Rincón de la Vieja crater lake show that rock dissolution and mineral precipitation/dissolution are the main processes that control the variability of cations composition over time. In particular, precipitation and dissolution of gypsum and alunite are responsible for the variations of REE in the waters. Despite the low variations of $(La/Pr)_{N\text{-local rock}}$ and $(LREE/HREE)_{N\text{-local rock}}$ ratios, this study allows to suggest that REE can be used, together with major elements, as practical tracers of water-rock interaction processes and mineral precipitation/dissolution at active hyperacid crater lakes over time, also during periods of quiescence and low phreatic activity.

KEYWORDS

rare earth elements (REE), hyperacid crater lake, geochemical monitoring, sulfate minerals, water-rock interaction

1 Introduction

In the past decades it has been largely demonstrated that the studies of the chemical composition of volcanic lakes, as well as the physico-chemical parameters, provide useful information about the variation of volcanic activity (Rowe et al., 1992; Christenson, 2000; Varekamp et al., 2000; Takano et al., 2004; Tassi et al., 2005; Tassi et al., 2009; Varekamp et al., 2009; Rouwet et al., 2017; Rouwet et al., 2019; Pappaterra et al., 2022). Volcanic lakes are intricated systems and their chemical composition can vary depending on the intertwining of natural processes that occur in these peculiar environments. Deep volcanic fluid input and water-rock interaction are the primary sources of anions and cations dissolved in the water, respectively (Henley and Ellis, 1983; Delmelle and Bernard, 1994; Varekamp, 2015; van Hinsberg et al., 2017). The different composition of lake waters and their variations over time depend on the type of gases and the variety of deposits and rocks that interact with the lake waters (Deocampo and Jones, 2014). Moreover, processes such as mineral precipitation, element vapor phase transport, variations in the input of meteoric waters, infiltration of lake water, sulfate reduction, induce changes in the lake volume and its chemical composition (Komor, 1992; Komor, 1994; Deocampo and Jones, 2014; Varekamp, 2015). Major and trace element variations over time allow to identify the main processes responsible for these changes as premonitory signals, and, in some cases, also to quantify their contribution.

Despite the fact that many studies deal with volcanic lake monitoring, most of these focus on the variations of major elements and of physico-chemical parameters. Some previous studies suggest that trace elements can also be used as geochemical tracers of water-rock interaction processes that occur at volcanic crater lakes. REE, for example, are sensitive tracers of rock dissolution and mineral precipitation processes. REE fractionation likely associated with the precipitation of gypsum/anhydrite and alunite was found in several volcanic-hydrothermal systems (Martínez, 2008; Varekamp, 2015; Inguaggiato et al., 2017; Inguaggiato et al., 2018; Inguaggiato et al., 2020a; Inguaggiato et al., 2020b; van Hinbserg et al., 2020; Pappaterra et al., 2022). Studying the geochemical behavior of REE at Poás's Laguna Caliente, it was observed that the differences in the ionic radii of REE lead to a differential incorporation during gypsum/anhydrite precipitation, that induce variations in their relative proportions over time and are related to varying activity of the underlying volcano-hydrothermal system (Inguaggiato et al., 2018; Pappaterra et al., 2022). Moreover, it was found that REE variations over time can reflect changes in volcanic activity of different volcanic-hydrothermal systems (Wood, 2006; Morton-Bermea et al., 2010; Varekamp, 2015; Pappaterra et al., 2022). Wood. (2006) found that the concentrations of REE in the crater lake of Mount Ruapehu (New Zealand) vary during 1993–1998 and these changes seem to be related to the phreatomagmatic eruption occurred in September 1995. Varekamp. (2015) found a relation with the decrease of La/Pr ratio in the thermal spring fluids of Copahue volcano (Argentina-Chile) and the occurrence of a volcanic eruption in 2000. The results obtained by Morton-Bermea et al. (2010) at El Chichón volcano (México), on the contrary, show that there were not important variations in the concentrations of REE during the period of observation, probably due to the steady conditions in the volcanic activity and the absence of volcanic eruptions. Recently, Pappaterra et al. (2022) found that the variations of REE dissolved in the active crater lake (Laguna Caliente) of Poás volcano (Costa Rica) are sensitive to the changes in the phreatic activity during a period of unrest occurred between 2009 and 2016. In particular, the highest values of ∑REE and La/Pr ratio and the lowest values of Light REE/Heavy REE (LREE/HREE; normalized to the average local rock) are associated with the period of most intense phreatic activity.

All these findings allow to propose that REE can be considered not only as tracers of the geochemical processes that usually occur at active crater lakes, but also as secondary geochemical tool used together with major elements and physico-chemical parameters, to detect the changes in the volcanic/phreatic activity. However, it is important to investigate more on the REE variations overtime in hyperacid crater lakes worldwide, in order to better understand the sensitivity of REE variations during the volcanic activity changes.

The present study investigates the major, minor, and REE elements as well as physico-chemical parameters in the active crater lake of Rincón de la Vieja volcano (Costa Rica) during the pre-unrest stage (February 2013 to August 2014) in order to: 1) investigate the response of major, minor and REE variations in relation to the phreatic activity, 2) define the REE geochemical behavior, 3) define the main water-rock interaction processes, and 4)

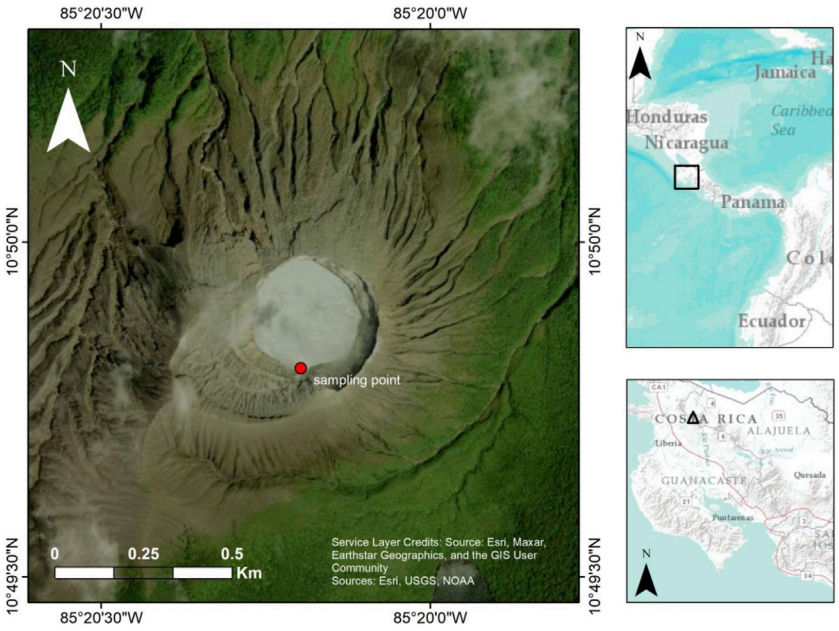

FIGURE 1
Map of Central America and location of Rincón de la Vieja volcano (black triangle). Detail of the active crater lake and location of the sampling point (red circle).

compare the REE variations and their fractionation in the Rincón de la Vieja crater lake, with those recently found in the Poás crater lake where more dynamic changes in volcanic activity occurred. This study contributes to increase the knowledge about the geochemical behavior of REE in hyperacid crater lakes, and their sensitivity to changes in volcanic activity.

2 Background information

2.1 Previous studies on geology and geochemistry of Rincón de la Vieja volcano

Rincón de la Vieja volcano (10.83°N 85.324°W; 1916 m above sea level) is one of the most active volcanoes in Costa Rica (Figure 1; Fung, 2008; Alvarado and Cárdenes, 2017; González et al., 2021). The area is characterized by the active subduction of the Cocos plate beneath the Caribbean plate (Alvarado and Cárdenes, 2017). Rincón de la Vieja is located in the NW of Costa Rica and it is part of the Guanacaste Volcanic Range (GVR), in the North-western part of the country (Kempter and Rower, 2000; Chavarria and Rodríguez, 2010; Alvarado and Cárdenes, 2017; Tassi et al., 2018). The chemical composition of the erupted products varies from basaltic andesite to dacitic; however, most of them have an andesitic composition (Soto et al., 2004).

Rincón de la Vieja, Miravalles and Tenorio volcanoes are part of the Guanacaste Geothermal Province (GTP; Giggenbach and Soto, 1992). In the three volcanoes there are acid sulfate hot springs, neutral chloride hot springs and fumaroles (Giggenbach and Soto, 1992; Kempter and Rower, 2000; Chavarria and Rodríguez, 2010; Tassi et al., 2018). A thermal reservoir identified on the south flank of Miravalles volcano allowed the construction of a geothermal powerplant, built and completed during the 90s (Giggenbach and Soto, 1992; Kempter and Rower, 2000).

The summit of Rincón de la Vieja volcano is characterized by the presence of numerous coalescent cones, one of them, the only active crater, hosts a hot hyperacid and hypersaline lake (Kempter and Rower, 2000) that has a chemical composition similar to Poás' Laguna Caliente (Rowe et al., 1992; Kempter and Rower, 2000; Tassi et al., 2005; Tassi et al., 2009; Delmelle et al., 2015; Rouwet et al., 2017; Rouwet et al., 2019). As previously found for similar volcanic hydrothermal systems, the major cations and anions chemical composition depend on gas input at the bottom of the lake from the magma body and the consequent dissolution of the andesitic rocks due to the high acidity of the waters (Kempter and Rower, 2000). Acid chloride-sulfate springs are located at the Northern flank of the volcano (Kempter and Rower, 2000; Tassi et al., 2005). Their chemical composition is coherent with the dilution of the brine by meteoric waters; these springs are supposed to be seeps from the crater lake (Kempter and Rower, 2000). Nevertheless, cation concentrations are higher with respect to those expected after dilution, which suggests an enrichment deriving from rock dissolution by the seeped brines. The dissolution of the volcanic deposits in the northern flank caused by the brines seeped from the crater lake is the primary cause of flank instability and the consequent collapse (Kempter and Rower, 2000; Delmelle et al., 2015).

The last large eruption occurred around 3.6 ky ago. The deposits associated, known as Río Blanco tephra, include a sub-plinian layer, with pumice and scoria (Kempter et al., 1996; Soto et al., 2004).

The eruptive mechanism was identified studying the chemical composition of these products, which can be explained with the involvement of a dacitic magma (Soto et al., 2004). The latter authors suggest that the intrusion of a new magma in the magma chamber,

with andesitic composition, could have been the trigger of the pyroclastic flow erupted 1.5 ka (Kempter et al., 1996; Soto et al., 2004). This andesitic magma is probably the one involved in the most recent and present volcanic activity (Soto et al., 2004).

2.2 Activity of Rincón de la Vieja volcano from 2013 to 2022

The information about the phreatic activity of Rincón de la Vieja during 2013–2022 here presented has been compiled using data from public sources (Red Sismológica Nacional, Universidad de Costa Rica, RSN:UCR-ICE, 2023; Observatorio Vulcanológico y Sismológico de Costa Rica, OVSICORI, 2022). The volcanic activity of Rincón de la Vieja volcano was stable and low during the period of observation of the current study, from February 2013 to August 2014. The period of unrest, which signed the start of the current phreatic activity (and also phreatomagmatic events) at the crater lake, began in 2015. The volcanic activity since 2015 counts more than 150 phreatic eruptions (2015–2022). Many of these events have been characterized by eruption columns with heights up to 2,000 m. Four phreatomagmatic eruptions occurred after 2015, often generating lahars on the north flank of the volcano that reached the Pénjamo river, affecting the local fauna. González et al. (2021) suggest that the large earthquake sequence of Central America in 2012 could have promoted an increase in the number of volcanic eruptions in the Central American Volcanic Arc (CAVA), including Rincón de la Vieja volcano.

During 2013, just one phreatic eruption has been observed and confirmed, on July 10th. The eruptive column of this phreatic eruption was only ~10 m high. White plumes rising from the active crater are reported on 26 February 2013. However, there were no seismic signals associated with a phreatic eruption. An important lake level drop was observed during February 2013 (−2.5 m with respect to the level measured in December 2012), coincident with a decrease in lake temperature. An intensification of the seismic signal has been recorded during August and November 2013, likely associated with fluids circulation. Moreover, sulfur spherules floating at the surface of the lake, proving the presence of a molten sulfur pool at the lake bottom, could probably be related with increased volcanic activity. Nevertheless, there are no phreatic events confirmed for the period August–November 2013. Considering that only one phreatic eruption was reported during the period of observation (February 2013–August 2014), we arbitrarily named this period as "low phreatic activity." Four phreatic eruptions are reported for 2014: three in September (17-19-20th) and another one at the end of October (24th). Unfortunately, in this study the crater lake was sampled until August 2014 thus it was not possible to compare the data about the chemistry of the crater lake with the activity occurred at the end of 2014.

3 Sampling and methods

3.1 Sampling

The crater lake of Rincón de la Vieja (Figure 1) was sampled eight times between February 2013 and August 2014. In each field trip, two samples of water were collected at the same sampling point, by throwing in a 1L sample bottle with a fishing rod from a ridge, 30 m above the lake surface. The samples were filtered *in situ* using Millipore filters with diameter of the pores of 0.45 μm and stored in 50 mL HDPE bottles. The samples were not acidified; acidification, in fact, is not necessary for hyperacid waters (pH ~ 0) like the ones hosted at Rincón de la Vieja crater lake. The temperature of the lake was measured with a digital thermometer immediately after retrieving the sample bottle, and pH was determined in the laboratory by titration using a NaOH solution (1M).

Variations in lake level were estimated from a scaled picture for each sampling campaign, except for November 2013, when the scaled picture was taken almost a month and a half later (December 12th). The changes in the lake level are here reported as the difference of the level (in m) with respect to reference level of April 2012.

3.2 Samples treatment

The water samples collected for chemical analyses, and stored in the HDPE bottles, were left in laboratory at a room temperature of ~22°C. The natural precipitation of secondary minerals occurred in four out of eight water samples (RVW4, RVW5, RVW6, and RVW8). The precipitated solid phases were separated by filtering the water sample using filters with a pore diameter size of 0.45 μm. A small part of all the solids was separated to carry out the chemical/mineralogical characterization with SEM-EDS. The remnants of the minerals precipitated were dried at 40°C for 24 h, grounded and dissolved using different amounts of HCl, HNO_3 and ultrapure H_2O, depending on the weight of the solid phase.

All the water samples and solid dissolved in the solution were diluted to reach a final salinity of ~0.6 g L^{-1}.

3.3 Analytical procedure and laboratory equipment

Crater lake waters and dissolved solid phases were analyzed for their major elements (Na, K, Ca, Mg, Si) at INGV-Palermo using an ICP-OES Ultima 2 (Horiba Jobin-Yvon): the concentrations of the elements are determined with quantitative methods using the calibration solutions in an opportune range for each element and calculating the weighted regression curve constructed with 10 calibration points. The concentrations of the elements in the analyzed samples are calculated with the spectrometer software (ICP Analyst, version 5.4). The accuracy of the analysis is validated analyzing different CRM solutions (NIST 1643e, SPS-SW1 and SPS-SW2) for each analytical session and never exceeds 10%. The precision (RSD) of analysis is calculated by three repetitions for each sample. Anion concentrations (Cl, SO_4, F) were determined by ionic chromatography (Dionex ICS 1100) previous opportune calibration performed on six levels in different ranges for each anion. Charge balance was calculated by PRHEEQC interactive software using THERMODDEM database and it is below 3%.

The concentrations of REE, Fe, Al, Ba and Sr were analyzed by ICP-MS Agilent 8,800 at "Sistema de Laboratorio Especializado de Ciencias de la Tierra" (SLE-CT) in the Centro de Investigación

Científica y de Educación Superior de Ensenada, Baja California (CICESE). The ICP-MS was calibrated with a calibration curve of 14 points ranging in concentration from 2.5 ppt to 2,000 ppb. A solution with ^{103}Rh, ^{115}In and ^{185}Re (internal standards) was used to monitor the sensitivity variation. The internal standard solution was added inline by a T piece that mixes the sample solution with the internal standard solution. The SPS-SW1 reference material was analyzed to evaluate the accuracy of the analysis. The accuracy of the REE is mostly <5%, while the accuracy of Fe, Al, Ba and Sr is <8%.

The mineralogical characterization of the solids precipitated was performed at the Università della Calabria (UniCal) through Energy Dispersion Microanalysis by Scanning Electron Microscope (SEM-EDS), using an Ultra High-Resolution SEM (UHR-SEM) - ZEISS CrossBeam 350, equipped with an EDS - EDAX OCTANE Elite Plus, Silicon drift type spectrometer (instrumental acquisition conditions: HV: 15 keV; Probe current: 100 pA; Working Distance: 11 mm, Take off: 40°, Time: 30 s).

3.4 Data treatment

The REE were subdivided in two sub-groups: 1) the sub-group of the Light Rare Earth Elements (LREE) including the elements from La to Gd, and 2) the sub-group of the Heavy Rare Earth Elements (HREE) including the elements from Tb to Lu, plus Y. $REE_{N\text{-local rock}}$ refers to the REE concentrations in the samples normalized to the REE average composition of the local volcanic rocks, mainly basaltic andesite and andesite rocks (Carr et al., 2013).

The two subgroups of REE can be differently affected by the processes that usually occur in hyper-acidic-hypersaline environments, like leaching from the volcanic rocks and the incorporation during mineral precipitation. The $(LREE/HREE)_{N\text{-local rock}}$ ratio is calculated using the following formula:

$$(LREE/HREE)_{N-local\,rock} = \sum LREE_{N-local\,rock} / \sum HREE_{N-local\,rock} \quad (1)$$

where $\sum LREE_{N\text{-local rock}}$ is the sum of the LREE concentrations in the samples, each element normalized to the LREE of the local volcanic rocks and $\sum HREE_{N\text{-local rock}}$ is the sum of the HREE concentrations in the samples, each element normalized to the HREE of the local volcanic rocks. The $(LREE/HREE)_{N\text{-local rock}}$ was used to identify water-rock interaction processes, as well as the dissolution of the primary rocks and precipitation/dissolution of secondary minerals. LREE, in fact, are preferentially incorporated during the precipitation of secondary minerals (gypsum/anhydrite, alunite, jarosite, barite) with respect to the HREE (Guichard et al., 1979; Deyell et al., 2005; Inguaggiato et al., 2018; Inguaggiato et al., 2020a; Inguaggiato et al., 2020b; van Hinsberg et al., 2020; Pappaterra et al., 2022; Cuadros et al., 2023). In particular, the results obtained studying the incorporation of REE in gypsum show a preferential incorporation of Pr with respect to the other LREE (Dutrizac, 2017; Inguaggiato et al., 2018; Inguaggiato et al., 2020a). This preferential incorporation is due to the similarity between Pr and Ca ionic radii in eightfold coordination in gypsum respect to the other LREE ionic radii (Dutrizac, 2017). Cuadros et al. (2023) studied the REE incorporation in alunite and jarosite minerals, finding that LREE are preferentially incorporated in both minerals with respect to HREE. In particular, the authors found a REE pattern decreasing from La to Lu for jarosite mineral and a preferential incorporation of Nd and Sm for alunite. This differential incorporation is due to the different size of the K-site in 12-fold coordination, larger for jarosite (Cuadros et al., 2023).

The $(LREE/HREE)_{N\text{-local rock}}$ and $(La/Pr)_{N\text{-local rock}}$ ratios here used to investigate about the variations of REE in the crater lake over time, allow to consider the effect of mineral precipitation and the consequent changes of REE at the crater lake during 2013–2014. In particular, the use of $(La/Pr)_{N\text{-local rock}}$ ratio allows to evaluate specifically the role of gypsum/anhydrite and its impact on REE behavior.

The correlation between all the variables (temperature, pH, major and minor elements, major elements ratios, TDS, ∑REE, and $(La/Pr)_{N\text{-local rock}}$ $(LREE/HREE)_{N\text{-local rock}}$ ratios in the lake waters) was tested with the Pearson's coefficient, using the following formula:

$$r = \sum [(X_i - \bar{X})(y_i - \bar{y})] / \sqrt{\sum (X_i - \bar{X})^2 * \sum (y_i - \bar{y})^2} \quad (2)$$

The value of r spans between −1 and +1 where r=|1| indicates a perfect (positive or negative) correlation while r=0 indicates that there is no relationship between the variables considered. The significance of the correlations was tested calculating the *p*-value. The correlation is considered significant if *p*-value <0.05.

4 Results

4.1 Physico-chemical parameters, major and minor elements of lake water

The major element composition and physico-chemical parameters of Rincón de la Vieja crater lake waters during the period 2013-2014 are reported in Table 1. The temperature varies from 28°C to 35°C, all the samples have pH < 0 that varies between −0.22 and −0.11. The Total Dissolved Solids (TDS) concentrations span from 82 to 115 g kg^{-1}. Supplementary Figure S1 shows the major element composition of the waters and their changes during the period of observation. It is noted that the major element composition varies during the period of observation. However, the variability of some major elements, particularly Ca, is slighter with respect to the variability found during long period of observation in similar active crater lakes (Rouwet et al., 2017; Pappaterra et al., 2022). Al is the cation with the highest concentrations that span from 5,920 to 8,415 mg kg^{-1}, followed by Fe and Na that varies from 2,286 to 3,668 and 1,403 to 2,221 mg kg^{-1}, respectively. Mg, K and Ca concentrations range from 953 to 1,533, 833 to 1,253, and from 863 to 1,037 mg kg^{-1}, respectively. Considering only the major and minor cations, Ba represents the one with the lowest concentrations that range between 0.08 and 0.13 mg kg^{-1}.

The anion composition is dominated by Cl and SO_4 with concentrations up to 34,694 and 59,013 mg kg^{-1}, respectively. The SO_4/Cl weight ratio varies in a narrow range from 1.7 to 1.9. Fluoride concentrations are one order of magnitude lower than

TABLE 1 Chemical composition of lake waters (mg kg^{-1}), TDS (g kg^{-1}) physico-chemical parameters and chemical composition of solid phases precipitated (wt%).

Chemical composition of the lake waters																
Sample	Date	T (°C)	pH	Na	K	Ca	Mg	Si	Al	Fe	Sr	Ba	F	Cl	SO_4	TDS
RVW4	13/02/2013	32.1	−0.22	2,221	1,254	959	1,533	53	8,416	3,538	28	0.076	3,467	34,694	59,013	115
RVW5	10/04/2013	30	−0.22	1,991	1,149	982	1,398	53	7,144	3,668	26	0.098	3,117	30,384	54,292	104
RVW6	16/07/2013	31.4	−0.11	1,451	833	1,037	1,059	66	5,940	2,486	23	0.083	2,366	23,773	43,031	82
RVW7	03/10/2013	35	−0.1	1,476	864	888	1,082	42	6,100	2,674	22	0.110	2,318	23,805	43,300	83
RVW8	12/12/2013	29	−0.11	1,403	833	1,009	1,041	52	5,920	2,940	22	0.085	2,269	23,300	43,317	82
RVW9	16/01/2014	29	−0.17	1,641	1,010	863	1,124	42	7,309	2,738	24	0.107	2,654	26,911	48,786	93
RVW10	24/04/2014	33	−0.21	1,796	1,085	870	1,255	40	7,188	3,031	23	0.079	2,804	29,202	54,668	102
RVW11	05/08/2014	28.4	−0.16	1,432	867	880	953	46	6,697	2,499	24	0.131	2,453	25,776	49,010	91
Chemical composition of the solid phase precipitated																
Sample	CaO	K_2O	MgO	Na_2O	SiO_2	Al_2O_3	Fe_2O_3	SrO	BaO	SO_3	Tot					
RVS4	37.0	1.00	0.105	0.90	0.50	1.12	0.511	0.119	0.0045	58.0	99.3					
RVS5	30.3	0.77	0.053	0.65	0.50	0.53	0.234	0.097	0.0062	45.8	79.0					
RVS6	29.1	0.72	0.009	0.51	0.43	0.09	0.032	0.093	0.0015	46.1	77.1					
RVS8	32.7	0.90	0.009	0.60	0.50	0.06	0.025	0.098	0.0017	51.2	86.1					

sulfate and chloride concentrations, from 2,269 to 3,467 mg kg^{-1}.

4.2 Chemical composition and mineralogy of the solid phase

The relative proportions of the major elements in the solid phase are reported in Table 1 and expressed as the weight percent of the corresponding oxide (wt%), calculated using the concentrations determined by ICP-OES in the solid phases dissolved in laboratory and analyzed by ICP-OES. The results show that all the samples are mainly composed of CaO (29%–37%) and SO_3 (46%–58%). The sum of all the other oxides is always minor than 5%. SEM-EDS analysis provided high-definition images and the chemical composition of the surface of the solids precipitated (Figures 2, 3). The main minerals precipitated, gypsum and anhydrite ($CaSO_4{\cdot}2H_2O/CaSO_4$), have elongated prismatic habit with uniform, smooth and homogeneous surfaces (Figures 2A, B). Gypsum/anhydrite crystals are also present as small aggregates (Figure 2C). The CaO and SO_3 wt% measured in several gypsum/anhydrite crystals with SEM-EDS are similar between the samples (~45% and ~55%, respectively). However, since SEM-EDS analysis does not allow to quantify the amount of water, it is not possible to discern if the mineral identified is gypsum or anhydrite. More likely all the samples are composed by variable amounts of both minerals as previously observed by Inguaggiato et al. (2020a) for the solids precipitated at Kawah Ijen crater lake (Java, Indonesia). The authors show in fact that the XRD analysis carried out on the solids precipitated at the crater lake of Kawah Ijen volcano confirms that various of the solid samples are mainly composed by gypsum (≥90%) and minor amounts of anhydrite (≤10%). The samples RVS4 and RVS6 show extended coating with bright to dark color on gypsum crystals (Figure 2D). The analysis of the coatings reveals that they are mainly composed by Al_2O_3 and SO_3, with minor amounts of Fe_2O_3, Na_2O, K_2O, CaO.

The high-definition images obtained with SEM-EDS reveal the presence of other minerals on the surface of gypsum/anhydrite crystals (Figure 3). These appear like minute isolated crystals (1–2 μm) or small aggregates (~5–20 μm) of sulfate minerals: 1) Al-sulfate often with low percentage of F (Figure 3A), 2) Fe, K-sulfate minerals (Figure 3B) 3) Ba, Sr-sulfate minerals (Figure 3C) and 4) Al-sulfate with significative amount of Mg around 10% (Figure 3D). Dark grey cubic or bipyramidal crystals of Al sulphate are particularly abundant in the sample RVS4 (Figure 3A). Fe, K-sulfate minerals were found in all the samples although they show a unique rosette pattern only in the sample RVS4 (Figure 3B). Isolated crystals of Ba, Sr-sulfate with acicular habit that sometimes form small aggregates were found in all the samples (Figure 3C). Al, Mg-sulfate minerals that show a peculiar fibrous habit were identified only in the samples RVS5 and RVS6 (Figure 3D). On the basis of the chemical composition and the habit of all the minerals identified, it is likely that they correspond to the following minerals: alunogen ($Al_2(SO_4)_3{\cdot}17(H_2O)$) or another hydrated Al sulfate, jarosite (K, $Fe_3(SO_4)_2(OH)_6$) and barite/celestine ($BaSO_4/SrSO_4$).

The results obtained with the SEM-EDS are coherent with the chemical composition of the dissolved solid phases analyzed by ICP-

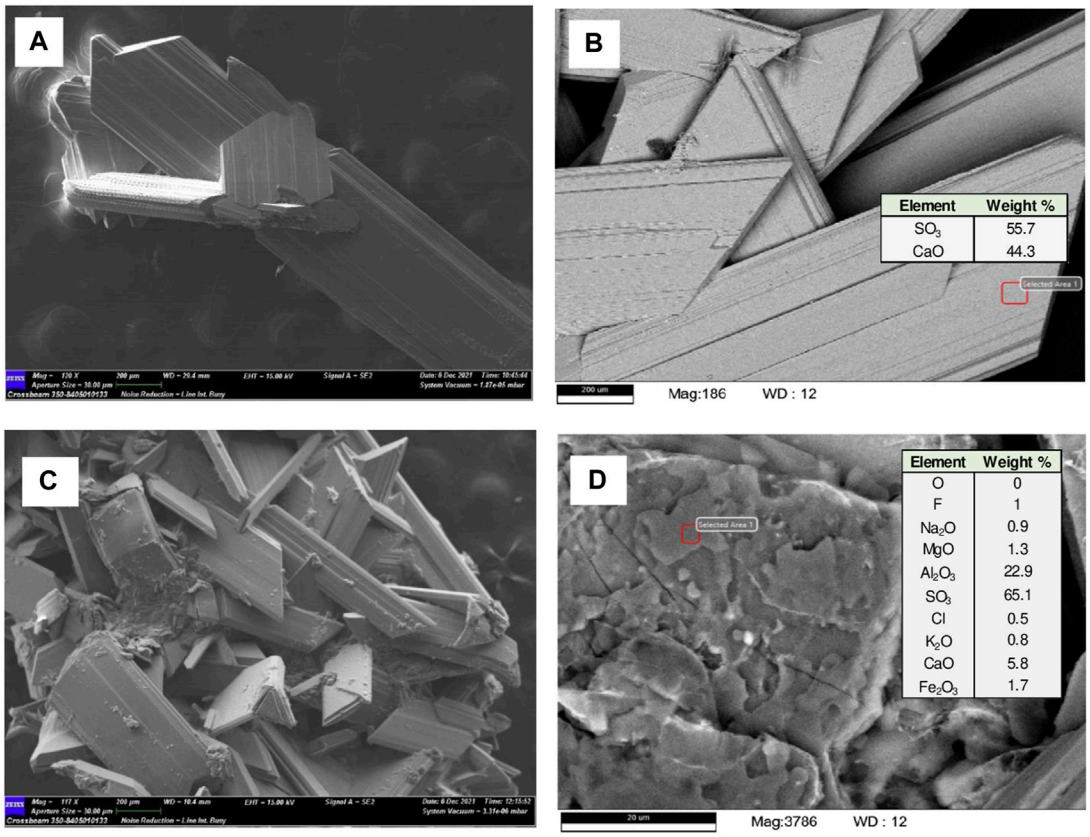

FIGURE 2
Gypsum/anhydrite crystals identified through SEM-EDS analysis. **(A)** isolated crystal of gypsum/anhydrite; **(B)** gypsum/anhydrite crystals and the relative chemical composition; **(C)** aggregates of gypsum/anhydrite crystals; **(D)** gypsum/anhydrite with extended coatings on the surface of the crystals and the relative chemical composition.

OES and ICP-MS, corroborating that the solid phases are mainly composed of Ca sulfate minerals (gypsum/anhydrite) and minor amounts (<5%) of other sulfates (Al, Fe and K, Ba, Sr sulfate minerals).

4.3 REE in waters and the solids precipitated

The total concentration of REE in water (∑REE) varies over time from 2.7 to 3.6 mg kg^{-1} (Table 2). REE concentrations normalized to the average composition of the local volcanic rocks (basaltic andesite and andesite rocks; Carr et al., 2013) show non-flat patterns, but LREE depleted patterns (Figure 4A). The ∑REE in the solids precipitated varies from 38 to 49 mg kg^{-1}. All the patterns of REE in the solid phases normalized to the local volcanic rock show, instead, LREE enriched patterns (Figure 4B).

The concentrations of the REE in the waters and the solids precipitated were used to calculate the distribution coefficient (K_D) for each element belonging to the REE, using the following formula:

$$K_D = [REE_i]_s / [REE_i]_{aq} \quad (3)$$

where $[REE_i]_s$ is the concentration of a selected REE in the minerals precipitated and $[REE_i]_{aq}$ represents the concentration of the same REE in the lake water from which the minerals precipitated. The results (Table 2; Figure 4C) show that the values of K_D are higher for LREE than HREE for all the samples. In particular, the values of the K_D increase from La to Nd. The latter and Pr have similar K_D values and are the REE with the highest K_D calculated. The values of K_D then drastically decrease from Sm to Lu.

4.3.1 Comparison of REE variations with major, minor elements and physico-chemical parameters over time

The $(La/Pr)_{N\text{-local rock}}$ and $(LREE/HREE)_{N\text{-local rock}}$ ratios were used to study the variations of REE patterns in crater lake water over time (Figure 5A) and to look at the processes that may have caused these variations, like leaching from the local volcanic rocks, dissolution and precipitation of secondary minerals. The $(La/Pr)_{N\text{-local rock}}$ ratio shows a low variability over time that ranges from 0.92 to 1.07 (Table 2; Figure 5A). The ratio decreases at the end of 2013 and then it rises at the beginning of 2014. The $(LREE/HREE)_{N\text{-local rock}}$ ratio varies between 0.66 and 0.81 and steadily increases throughout the considered period. The variations of the two ratios are compared with the variations of ∑REE over time (Figures 5B, C). It is observed that ∑REE decreases during the first

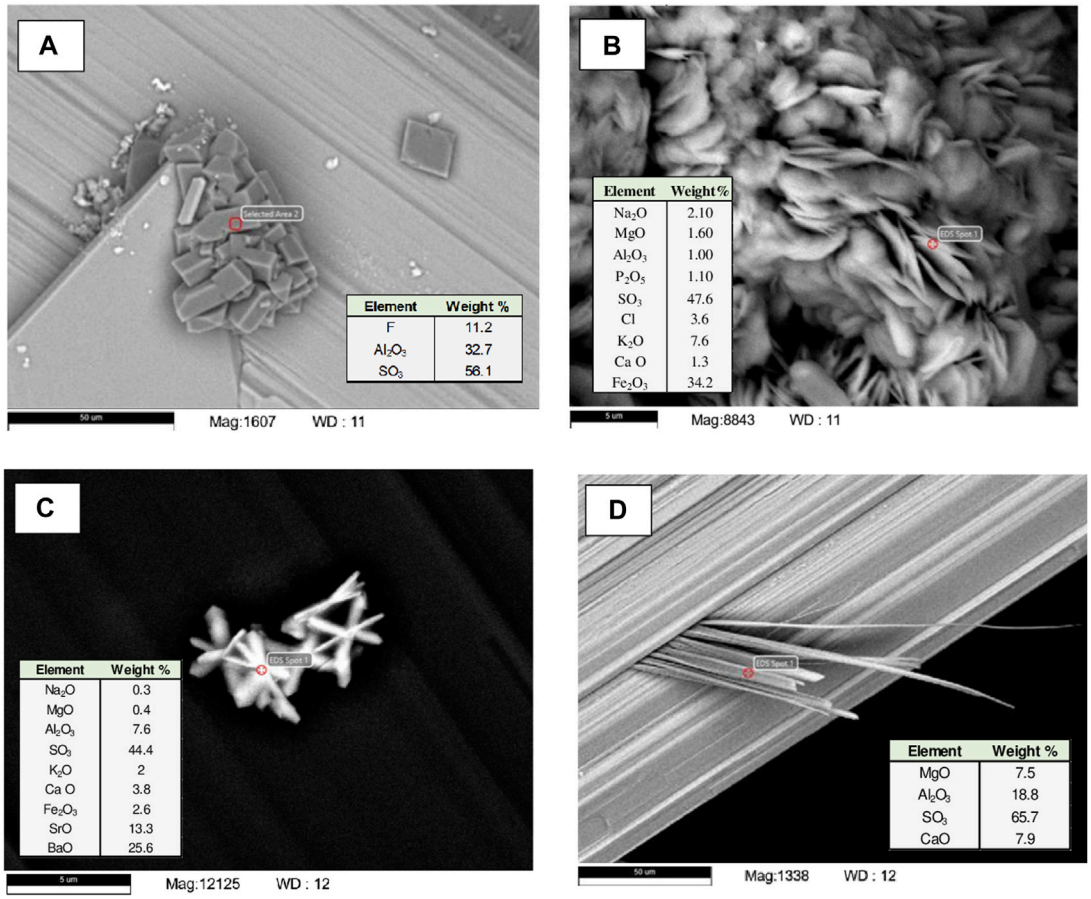

FIGURE 3
Sulfate minerals on gypsum/anhydrite crystals identified with SEM-EDS analysis and the relative chemical composition: **(A)** Al-sulfate; **(B)** jarosite; **(C)** baryte; **(D)** Al, Mg-sulfate.

half of the period considered until 2.8 mg kg^{-1} in July 2013, then it slightly increases until 2.9 mg kg^{-1} in October 2013 and then decreases again and reaches the lowest value (2.7 mg kg^{-1}) at the end of the year. On the contrary, the ∑REE increases during the second half of the period of observation and reaches 3.2 mg kg^{-1} at the end of August 2014.

The correlations calculated between $(La/Pr)_{N\text{-local rock}}$, $(LREE/HREE)_{N\text{-local rock}}$ and ∑REE are not significant, and they are equal to −0.17 and −0.37 respectively (Figure 5; Supplementary Table S1). The correlation between $(La/Pr)_{N\text{-local rock}}$ and $(LREE/HREE)_{N\text{-local rock}}$ ratios is equal to 0.16. However, it can be observed that ∑REE show values of the correlation coefficient >0.67 with all the major elements, except Ca, Si and Ba.

The correlation between the variations of $(La/Pr)_{N\text{-local rock}}$ and $(LREE/HREE)_{N\text{-local rock}}$ and the variations of major and minor elements (Na, K, Mg, Ca, Al, Fe, Si, Ba, Sr, S, Cl, F), Mg/Cl and SO_4/Cl ratios and physico-chemical parameters over time were calculated (Supplementary Table S1). The results show that the correlation between $(La/Pr)_{N\text{-local rock}}$ ratio over time, the variations of major elements, their ratios and physico-chemical parameters vary from |0.03| and |0.43|. The correlation is higher for $(LREE/HREE)_{N\text{-local rock}}$ ratio with values that span from |0.38| and |0.81| (Supplementary Table S1). The correlations calculated between the cations, anions and $(LREE/HREE)_{N\text{-local rock}}$ variations show the highest values for K (−0.64), Na (−0.73), Fe (−0.75) and Mg (−0.81). Moreover, all the correlations are negative except for Ba (0.52). However, it is important to specify that the only significant values of the Pearson's coefficient are those calculated between $(La/Pr)_{N\text{-local rock}}$ and temperature, and between $(LREE/HREE)_{N\text{-local rock}}$ and Na, Mg, Fe, Mg/Cl and SO_4/Cl. Regarding the behavior of the major elements it is noted that almost all the major anions and cations behave similarly except Ca, Ba and Si. Their variations over time are in fact different with respect to the variations of all the other elements considered. For this reason, the variations of all the major elements over time, except Ca, Ba and Si, are here represented by the pattern of TDS over time (Figures 6A, B). The different behavior of Ca, Si and Ba (and their patterns over time; Figures 7A–F) is also congruent with the values of their correlation coefficients (Supplementary Table S1). Looking at the results obtained, in fact, the correlation coefficients calculated between all the major elements (except Ca, Si and Ba) vary between |0.66| and |0.98| while the correlation coefficients calculated between Ca, Si, and Ba and the other major elements are always lower than |0.4|. Ca and Si

TABLE 2 REE concentrations in waters and solid phases precipitated (μg kg-1), and the REE distribution coefficients calculated.

Sample	La	Ce	Pr	Nd	Sm	Eu	Gd	Tb	Dy	Y	Ho	Er	Tm	Yb	Lu	Tot	$(La/Pr)_{N\text{-}local\ rock}$	$(LREE/HREE)_{N\text{-}local\ rock}$
REE concentrations in waters																		
RVW4	456	1,160	136	532	109	31	127	19	111	686	25	81	13	95	16	3,596	1.00	0.66
RVW5	437	1,119	130	507	103	30	122	18	106	619	24	77	12	89	15	3,406	1.00	0.67
RVW6	385	933	112	435	86	25	97	14	83	490	18	60	9	69	12	2,830	1.02	0.72
RVW7	363	998	118	456	90	27	104	15	88	484	19	63	10	72	12	2,917	0.92	0.73
RVS8	385	928	108	418	81	23	92	13	78	460	17	56	9	65	11	2,745	1.07	0.75
RVW9	429	1,081	124	477	92	27	107	15	90	516	20	67	11	75	13	3,143	1.03	0.74
RVW10	428	1,132	131	516	105	29	115	16	96	536	21	67	10	77	13	3,292	0.97	0.77
RVW11	452	1,130	132	514	101	28	110	16	91	510	20	63	10	71	12	3,258	1.02	0.81
REE concentrations in solids precipitated																		
RVS4	6,281	21,260	2,916	11,866	1,850	397	1,225	134	564	1,988	93	250	23	148	17	49,012		
RVS5	5,258	16,797	2,250	8,964	1,357	286	900	90	382	1,274	60	168	17	93	11	37,905		
RVS6	4,731	16,965	2,291	8,938	1,348	287	895	96	386	1,261	64	161	15	72	10	37,520		
RVS8	6,127	22,302	3,023	11,866	1,748	354	1,082	106	412	1,266	65	180	16	89	10	48,645		
REE distribution coefficients K_D																		
RVS4	13.85	18.44	21.61	22.52	17.12	12.72	9.71	7.21	5.11	2.90	3.74	3.08	1.80	1.55	1.10			
RVS5	12.17	15.23	17.60	17.99	13.34	9.78	7.44	5.13	3.63	2.06	2.55	2.19	1.37	1.04	0.77			
RVS6	12.43	18.48	20.73	20.91	15.85	11.78	9.26	6.85	4.65	2.58	3.53	2.70	1.54	1.04	0.82			
RVS8	16.09	24.47	28.62	29.00	21.86	15.50	11.91	8.34	5.31	2.76	3.79	3.21	1.85	1.36	0.93			

are well correlated (0.92) also shown with similar temporal variations (Figure 7 a, 7b, 7c, 7d). Analyzing in detail all the patterns (Figures 6 and 7) we can observe that the major elements (represented by TDS pattern), except Ca, Si and Ba (Figures 6, 7) are characterized by high concentrations in March 2013, which then decrease abruptly and successively remain quite constant during the year.

No clear correlation is observed between the major, minor elements and physico-chemical parameters and $(La/Pr)_{N\text{-}local\ rock}$, $(LREE/HREE)_{N\text{-}local\ rock}$ and ∑REE (Supplementary Table S1). However, the ∑REE is highly correlated with TDS (Supplementary Figure S2), almost all the major cations (except Ca, Fe, Si and Ba) and the major anions variations over time ($r \geq 0.77$). Finally, there is no relation between the values of ∑REE, $(La/Pr)_{N\text{-}local\ rock}$ and $(LREE/HREE)_{N\text{-}local\ rock}$ ratios and the phreatic eruption occurred on July 10th.

4.4 Rainfall *versus* lake level fluctuations

In terms of climate, northwest Costa Rica is affected by a dry season, from January to April, and a wet season, from May to December (Alvarado and Cárdenes, 2017; Instituto Meteorológico Nacional, 2022).

Supplementary Figures S3A, B shows the monthly rainfall (in mm) and variations in crater lake level for the period April 2012–September 2014 (reports, Instituto Meteorológico Nacional, 2022). An anomalous amount of rain was reported during April 2012 (125 mm), compared with April 2013 (0 mm) and April 2014 (4.9 mm). During the wet season of 2012, the quantity of rain varied from 1 mm (December) to 235 mm (September). No anomalous data of rainfall are reported during the dry season of 2013 compared to the previous year. The total amount per month of mm during the wet season is higher in 2013 (1,741 mm) with respect to the wet season of 2012 (1,360 mm). According to the amount of rain reported during the preceding years, also in 2014, the quantity of rain during the dry season is low (4.9 mm from January to April). The wet season of 2014 is characterized by lower rainfall with respect to the previous years during the period from May to August. However, in September 2014 the highest amount of rain (425 mm) is recorded.

The variations of the lake volume are reported as the relative variation of the lake level over time (m) compared to point "0", which corresponds to the level measured in April 2012. Supplementary Figure S3 shows that the lake level decreases throughout the entire period of observation. In particular, it decreases during the wet season of 2012 and remains stable

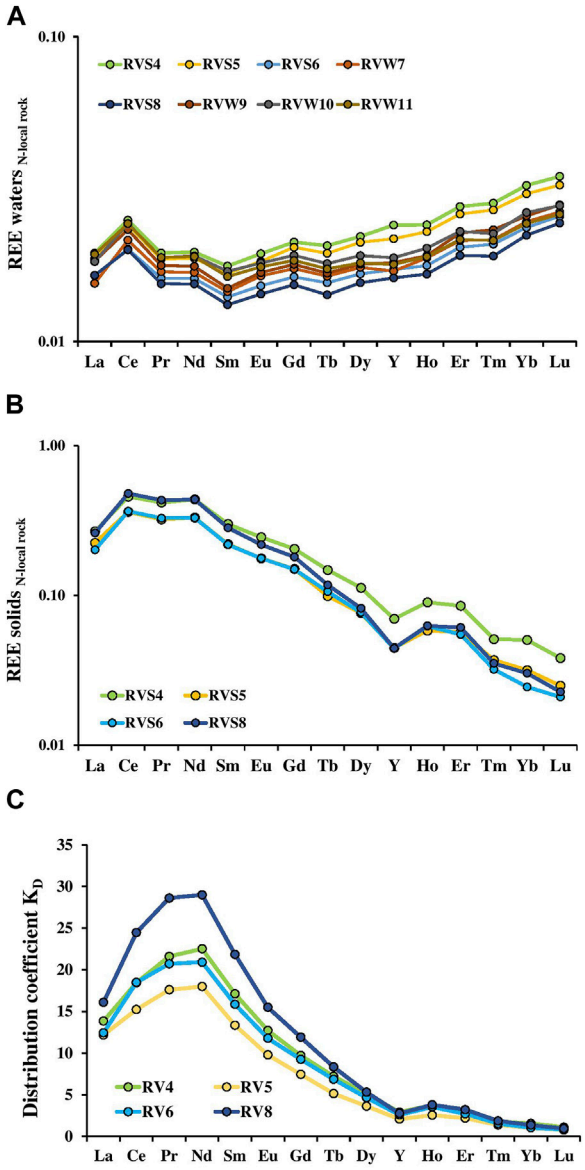

FIGURE 4
(A) REE patterns of the lake waters normalized to the local volcanic rocks; **(B)** REE patterns of the solids precipitated (mainly gypsum/anhydrite) normalized to the local volcanic rocks; **(C)** REE distribution coefficients (K_D) calculated between solids precipitated (mainly gypsum/anhydrite) and the lake waters of Rincon de la Vieja.

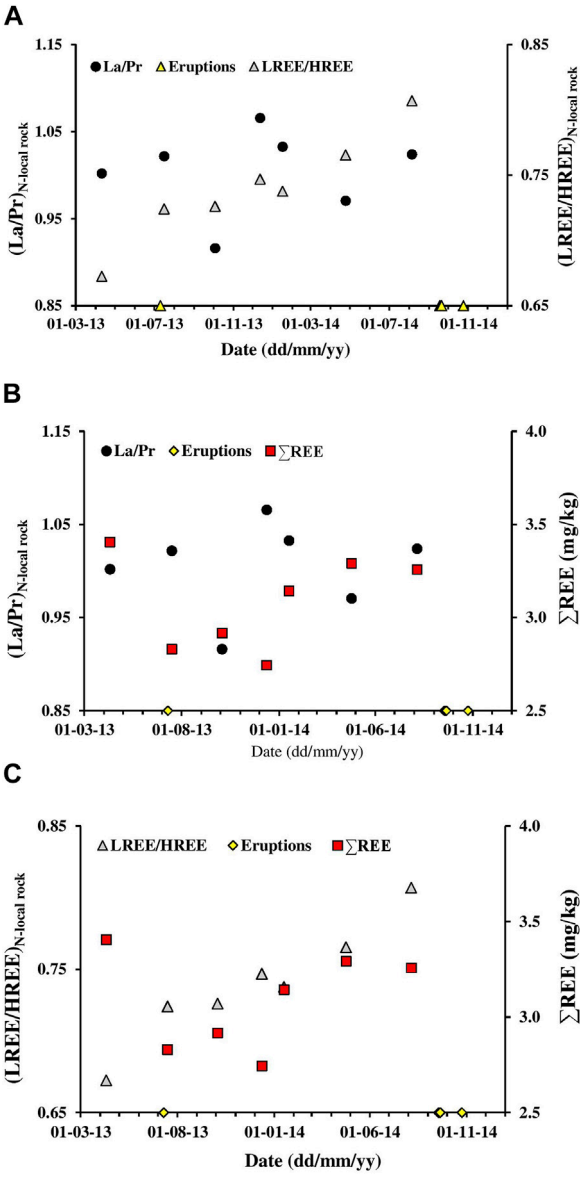

FIGURE 5
(A) $(La/Pr)_{N\text{-local rock}}$ and $(LREE/HREE)_{N\text{-local rock}}$ variations in crater lake waters vs. time; **(B)** $(La/Pr)_{N\text{-local rock}}$ and ∑REE variations in crater lake waters vs. time; **(C)** $(LREE/HREE)_{N\text{-local rock}}$ and ∑REE variations in crater lake waters vs. time.

at −0.5 m during September and December 2012. The decreasing trend continued during the dry season of 2013, to reach −3.5 m in late-April 2013. Due to the lack of data between May and September 2013 it is not possible to quantify the fluctuations of the lake level. However, the observed lake level is higher in October 2013 compared the previous measurement (−2.5 m). The only data available for the 2014 dry season are at the end of April, when the level drops, to reach the lowest level during the entire period of observation corresponding to −4.25 m. Afterwards, the lake level rises again during the wet season, up to −3.5 m.

5 Discussion

5.1 Major and minor elements variations in lake water and geochemical processes over time

The chemical composition and physico-chemical parameters of active crater lakes can provide important information about the volcanic activity (Christenson, 2000; Varekamp et al., 2000; Varekamp et al., 2009; Rouwet et al., 2017; Rouwet et al., 2019). The low variability of the water temperature (28.4°C—35°C; Table 1) at Rincón de la Vieja crater lake suggests that during the period of

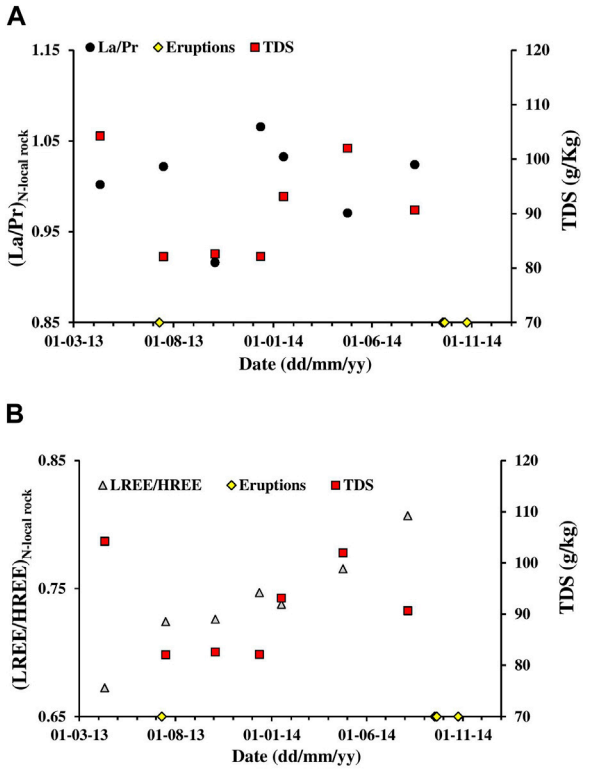

FIGURE 6
(A) $(La/Pr)_{N\text{-local rock}}$ and TDS variations vs. time; **(B)** $(LREE/HREE)_{N\text{-local rock}}$ and TDS variations vs. time.

observation the volcano was characterized by relatively stable and low phreatic activity, as confirmed by the negligible number of phreatic eruptions. The occurrence of a phreatic eruption on 10 July 2013, is not preceded by an increase in anion concentrations, neither by an increase of the lake temperature, parameters that can generally reflect an increase in the gas input. On the contrary, the concentrations of SO_4, Cl and F in the lake started to decrease at the beginning of 2013 and dropped just after the occurrence of the phreatic eruption of 10 July 2013. The concentrations increased during 2014 and then decreased again before the phreatic eruptions of September 2014 (Table 1).

The ISOSOL plot (Inguaggiato et al., 2015; Varekamp, 2015; Inguaggiato et al., 2020a; Inguaggiato et al., 2020b) was used to investigate the processes that affect the variations of major and minor elements over time in the crater lake of Rincón de la Vieja (Figures 8A–H). The ISOSOL plot allows to compare the chemical composition of the lake waters with that of the rocks which they are interacting with. This plot allows to identify the main water-rock interaction processes that could be responsible for the fluid chemistry. However, since the congruent rock dissolution line is graphically estimated, it implies that the method is characterized by a certain grade of arbitrariness. The chemical composition of the local volcanic rocks used for the ISOSOL plot is the average chemical composition of andesitic rocks and andesitic scoria deposits forming the crater wall (Alvarado and Cardenes, 1985; Soto et al., 2004; Carr et al., 2013; Supplementary Table S2). Plotting the chemical composition of each water vs. the average composition of the local volcanic rocks, it was possible to estimate the amount of rock dissolved for each sample, element by element (Figure 8). The ISOSOL plots show that most of the major elements lie on or near the congruent dissolution line for all the samples (Figures 8A–H). Al and Na, instead, are always slightly enriched in the water with respect to the rock (Al and Na excess), whereas Ca, Ba, and Si are always depleted (Ca, Ba, Si loss). Considering only the aligned elements, it is possible to estimate the quantity of local volcanic rock dissolved in the crater lake water, ranging from 160 g kg^{-1} in early-February 2013 to 110 g kg^{-1} in late-2014 (Figure 8; Table 3). The Al excess can be explained by the re-dissolution of Al-bearing minerals, like alunite, probably precipitated at the bottom of the lake or in the underlying hydrothermal system. The concomitant excess of Na could be related to the type of alunite mineral, mainly natro-alunite. The K/Na and Al/Fe ratios in waters were compared with those in the average local volcanic rocks (0.70 and 1.64, respectively). The K/Na ratio in the waters spans from 0.56 to 0.61 (the ratio slightly increases throughout the period of observation), while Al/Fe in the waters varies from 1.95 to 2.68. The finding of different values of the K/Na and Al/Fe ratios in the waters respect to the same ratios in the average local rock allows to propose that additional processes, more than the iso-chemical dissolution of the local volcanic rocks, control the concentrations of these cations in the waters. Specifically, the lower K/Na ratio and the higher Al/Fe ratio in the waters with respect to the same ratios in the average local volcanic rock, could support the redissolution of natro-alunite suggested with the ISOSOL plot. Beyond the redissolution of natro-alunite, these findings could also coincide with jarosite precipitation. The precipitation of jarosite in the crater lake is supported, in fact, by the SEM-EDS analysis that allow to identify various sulfates on gypsum/anhydrite crystals, jarosite among them (Figure 3B). Looking at the cations that show a depletion with respect to the near congruent rock dissolution line, the lower concentrations of Ba and Si in the waters suggest the precipitation of barite and silica, respectively. The depletion in Ca (Ca loss) is consistent with the precipitation of Ca-bearing minerals like gypsum/anhydrite, as found in the analysis of the solid phase precipitated in laboratory in some of the water samples (Figure 2; Table 1), and at other craters lakes like those of Poás (Inguaggiato et al., 2018; Pappaterra et al., 2022) and Kawah Ijen (Java, Indonesia; Inguaggiato et al., 2020a; van Hinsberg et al., 2020). In particular, XRD analysis of the solid precipitated in laboratory from the water sampled at Poás crater lake (Inguaggiato et al., 2018) shows that gypsum is the main mineral. Similarly, the XRD and SEM-EDS analysis carried out on the solids precipitated in laboratory from the Kawah Ijen hyperacid crater lake (Inguaggiato et al., 2020a) shows that gypsum and minor amounts of anhydrite are the main minerals precipitated. Minor amounts of Al-sulfate, jarosite, barite and celestite are identified on the surface of the main crystals, as also identified in this study. These results fit the experimental data on the precipitation of secondary minerals due to the evaporation of hyperacid brines (Gamazo et al., 2011; Toner et al., 2015; Rodríguez et al., 2018), showing that gypsum/anhydrite are the first minerals to precipitate followed by sulfates composed of Al, Fe, Na, and K, like the minerals identified at Kawah Ijen crater lake (Inguaggiato et al., 2020a) and in this investigation. Despite the slight variation of pH during 2013–2014, the role of pH, as well as temperature, cannot be excluded in controlling the mineral assemblage at the crater lake. The existence of a relation between the acidic conditions of the waters and the mineral assemblage has been well documented in the past (Miller et al., 2014; Rodríguez and

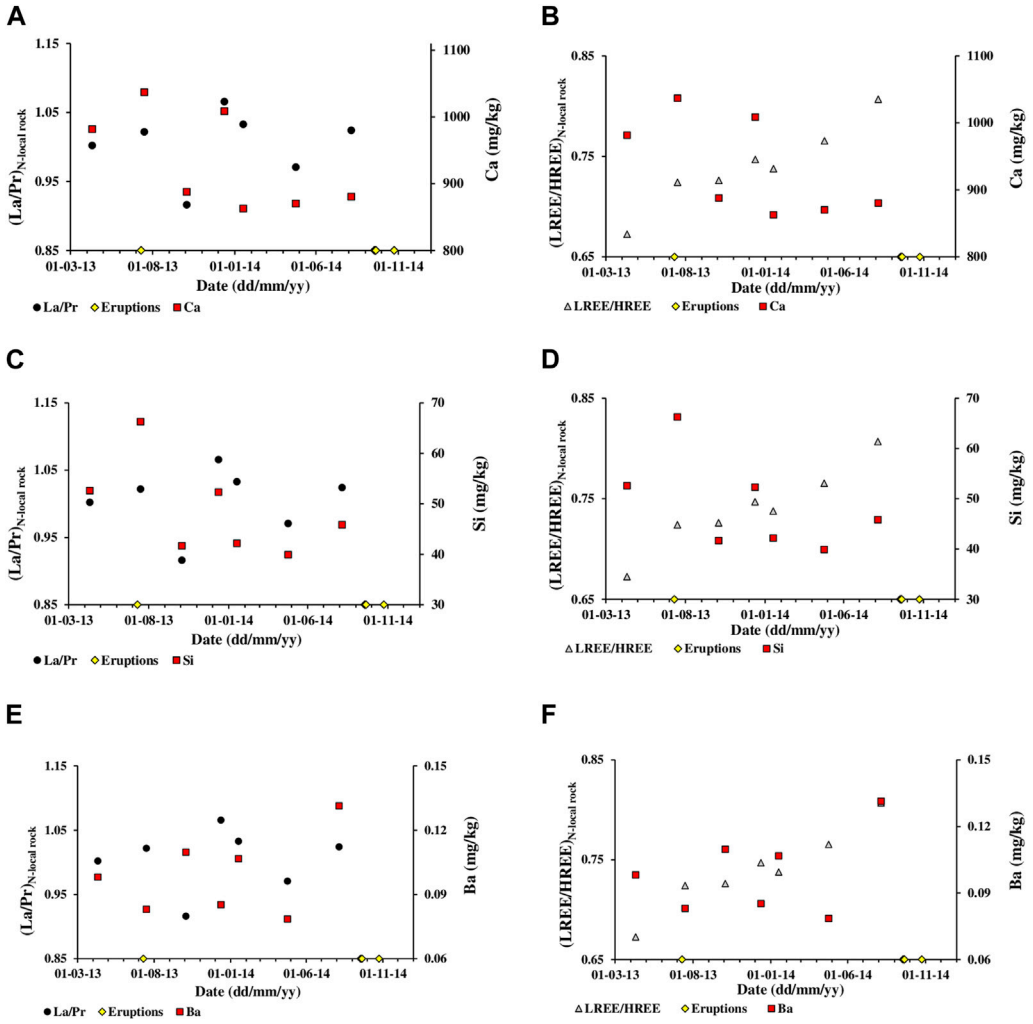

FIGURE 7
(A) $(La/Pr)_{N\text{-local rock}}$ and Ca vs. time; **(B)** $(LREE/HREE)_{N\text{-local rock}}$ and Ca vs. time; **(C)** $(La/Pr)_{N\text{-local rock}}$ and Si vs. time; **(D)** $(LREE/HREE)_{N\text{-local rock}}$ and Si vs. time; **(E)** $(La/Pr)_{N\text{-local rock}}$ and Ba vs. time; **(F)** $(LREE/HREE)_{N\text{-local rock}}$ and Ba vs. time.

van Bergen, 2017; Rodríguez et al., 2018). In particular, Rodríguez et al. (2018) found that some sulfate minerals like alunite and jarosite only precipitate under specific pH conditions (pH < 4). The changes in some lake parameters, for example, the increase of temperature and pressure at depth could lead to the precipitation of other sulfate minerals (Rodríguez and van Bergen, 2017), or even the precipitation of major amounts of alunite and jarosite, as proposed for Poás and Rincón de la Vieja volcanoes (Martínez, 2008; Ayres, 2012). The existence of a mineral assemblage in the hydrothermal system beneath the lake, including natro-alunite, gypsum and anhydrite, was proposed to explain the crater lake dynamics and the evolution of the volcanic activity at Ruapehu (New Zealand; Christenson et al., 2010). This type of minerals assemblage can act as a seal, that generates high pore pressure and accumulation of gases, leading to important gas driven phreatic eruptions, as experienced at Ruapehu crater lake in September 2007 (Christenson et al., 2010). Mineral accumulation and dissolution could have led to the creation of a similar mineral assemblage in the hydrothermal system of Rincón de la Vieja volcano, inducing changes in the underlying system, probably accountable of the phreatic activity changes of the unrest period subsequent to the period of observation of this investigation.

5.2 REE variations and their relation with major elements and physico-chemical parameters over time

The results presented in paragraph 4.3 show that the total amount of REE in waters varies over time (2.7–3.6 mg kg^{-1}). However, all the water samples show similar $(REE)_{N\text{-local rock}}$ patterns (Figure 4A) characterized by $(LREE/HREE)_{N\text{-local rock}}$ ratios ranging from 0.66 to 0.81. The $(REE)_{N\text{-local rock}}$ patterns of the solids precipitated in laboratory from the lake waters exhibit an enrichment in LREE with respect to HREE (Figure 4B). The LREE enrichment indicates that LREE are preferentially incorporated in secondary minerals that precipitate in the crater lake, probably the same identified through SEM-EDS analysis in the solids precipitated in laboratory from the lake waters (gypsum/

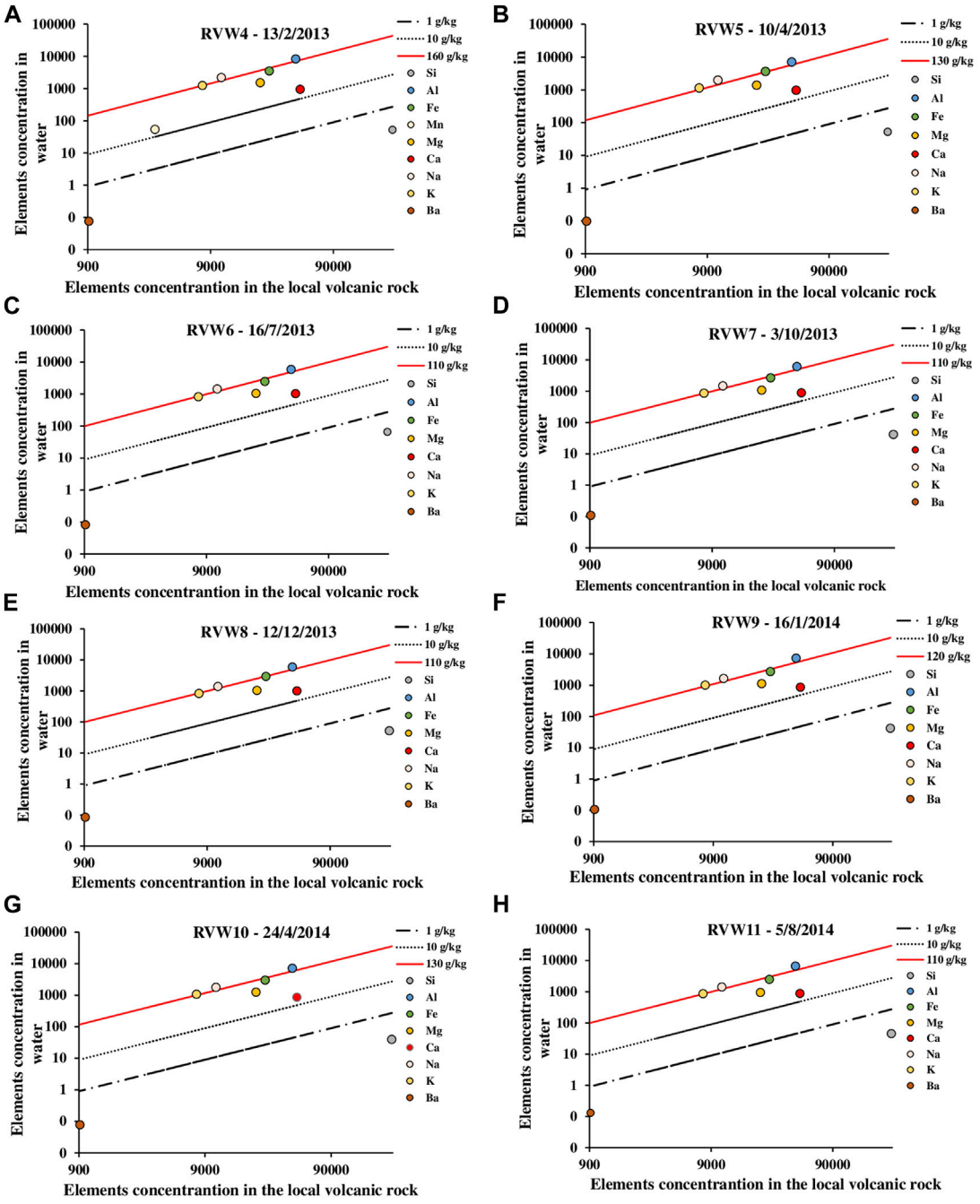

FIGURE 8
ISOSOL plots of elements in the local volcanic rock and dissolved in crater lake waters (ppm), for each sample (Figures **A–H**). The red line is indicative of the amount of rock dissolved per kg of water. Almost all the cations lie near the congruent dissolution line except Ca, Ba, and Si that are always depleted (Ca, Ba and Si loss), while Al and Na are always slightly enriched (Al, Na excess).

anhydrite and minor amounts of Al-sulfate, jarosite, barite and celestine).

Previous studies about the incorporation of REE in different sulfate minerals (gypsum, alunite, barite; Guichard et al., 1979; Deyell et al., 2005; Ehya and Mazraei, 2017; van Hinsberg et al., 2020) show that LREE are preferentially incorporated with respect to MREE and HREE. As mentioned in paragraph 3.4, the substitution of LREE in gypsum crystals is favored by the similarity between LREE and Ca (1.12 Å) ionic radii in eightfold coordination, in particular Pr (1.126 Å; Shannon and Prewitt, 1969). The main mechanism proposed for REE incorporation in gypsum crystals is the substitution in the crystal lattice of $2REE^{3+} + \square = 3Ca^{2+}$, where "□" corresponds to a vacant Ca site (Dutrizac, 2017; Lin et al., 2019). The preferential incorporation of LREE in sulfate minerals, in particular gypsum crystals, is corroborated by the REE distribution coefficients (K_D) calculated between the solid phase precipitated in laboratory and the waters from which gypsum precipitated (Figure 4C). The results in Table 2 show that the K_D

TABLE 3 Values of Ca loss (Ca*), Al and Na excess (Al*, Na*). The amount of rock dissolved (g per kg of lake water) was estimated using the ISOSOL plots. The amounts of gypsum precipitated and alunite dissolved were calculated using the values of Ca* and Al* respectively.

Sample	Date	Ca* (ppm)	Al* (ppm)	Na* (ppm)	Rock dissolved (g per liter of water)	g of gypsum precipitated	g of alunite redissolved
RVW4	13/02/2013	6,757.2	−1,323.9	−461.1	160	29.1	6.7
RVW5	10/04/2013	5,287.6	−1,382.3	−561.2	130	22.8	6.7
RVW6	16/07/2013	4,267.6	−1,064.0	−241.6	110	18.4	5.1
RVW7	03/10/2013	4,417.0	−1,224.4	−265.8	110	19.0	6.2
RVW8	12/12/2013	4,296.0	−1,044.9	−193.1	110	18.5	5.1
RVW9	16/01/2014	4,924.2	−1990.4	−321.2	120	19.1	9.8
RVW10	24/04/2014	5,399.0	−1,426.0	−366.3	130	23.2	7.2
RVW11	05/08/2014	4,424.3	−1,821.2	−222.1	110	19.0	9.2

values of LREE are higher compared to the HREE, with a peak in correspondence of Pr and Nd. Similar K_D patterns were also found in Poás and Kawah Ijen crater lakes where it was found that gypsum/anhydrite are the main minerals responsible for REE fractionation in the hyperacid crater lake. Nevertheless, the precipitation of the other sulfates like Al-sulfate, jarosite, barite and celestine cannot be excluded (Inguaggiato et al., 2018; Inguaggiato et al., 2020a; van Hinsberg et al., 2020).

As observed at similar hyperacid crater lakes (Wood, 2006; Varekamp et al., 2009; Varekamp, 2015; Inguaggiato et al., 2018; Pappaterra et al., 2022) the REE temporal variations in the Rincón de la Vieja crater lake seem to be related to two main processes: 1) the leaching of the local volcanic rocks, and 2) precipitation and dissolution of secondary minerals.

In this study, the REE variations have been compared with the volcanic activity of Rincón de la Vieja volcano for the period 2013-2014 (Figure 5). During this period the volcano was mainly in a state of quiescence, with only infrequent phreatic activity. $(La/Pr)_{N\text{-local rock}}$ and $(LREE/HREE)_{N\text{-local rock}}$ ratios are not correlated and do not show any relation with the changes in volcanic activity (Figure 5A; Supplementary Table S1). The $(LREE/HREE)_{N\text{-local rock}}$ ratio increases throughout the period of observation. This behavior could be the effect of the precipitation and/or dissolution of secondary minerals over time, as well as the variations of the amount of volcanic rock leached by the hyperacid waters. The increasing trend hence suggests that, beyond the precipitation of secondary minerals (like gypsum/anhydrite and other sulfates), probably the dissolution of alunite, mainly containing LREE with respect to HREE, could be responsible for the increase of $(LREE/HREE)_{N\text{-local rock}}$ over time. The ∑REE is highly correlated with pH, TDS, almost all the major cations (correlation ≥0.77; except Ca, Fe, Si and Ba) and the major anion variations over time (Supplementary Table S1). Despite the slight variability of pH during 2013–2014, the high correlation between ∑REE and pH (Supplementary Table S1) suggests that the leaching of REE over time is controlled by the acidity conditions of the lake, whose variations are induced by the mutable gas input at the bottom of the lake.

As mentioned in Section 4.3.1, $(LREE/HREE)_{N\text{-local rock}}$ ratio is highly correlated with SO_4/Cl over time (0.93; Supplementary Table S1; Supplementary Figure S4). In fact, similarly to $(LREE/HREE)_{N\text{-local rock}}$ ratio, also SO_4/Cl ratio increases through the entire period considered suggesting an enhancement in the SO_2 input with respect to HCl. However, the non-conservative behavior of HCl in hyperacid waters could affect the relative proportion between the two species over time (Rouwet et al., 2014; Rouwet et al., 2017). The increasing SO_4/Cl ratio during 2013–2014 may be associated with an increase in the gas input prior to the unrest started in 2015.

In relation to the activity of the volcano, the evaporation of crater volcanic lakes as well as variations in the climatic conditions can induce changes in the volume of the crater lake and thus the chemistry of the waters (DeoCampo and Jones, 2014). A lake level decrease is observed from 2012 to 2014 (Supplementary Figure S3), reaching a minimum of almost −4.5 m under the reference level (April 2012); however, the main variations of the lake level are coherent with the alternation of the dry and wet seasons. In Figures 9A, B, Figures 10A–C, the variations of the lake level are compared with the variations of TDS (g kg^{-1}), Ca (mg kg^{-1}), ∑REE, $(La/Pr)_{N\text{-local rock}}$ and $(LREE/HREE)_{N\text{-local rock}}$ ratios. Values of TDS are high during the dry season and low during the rainy season, which reflects a dilution effect by rainfall (Figure 9A). The ∑REE concentrations (Figure 10A) show a similar trend as TDS, explained by the alternation of dry and rainy seasons, whereas the $(La/Pr)_{N\text{-local rock}}$ ratio (Figure 10B) behaves similarly as the variation in Ca concentration. The $(LREE/HREE)_{N\text{-local rock}}$ ratios do not seem to be affected by the changes in lake level, particularly after mid-2013 (Figure 10C).

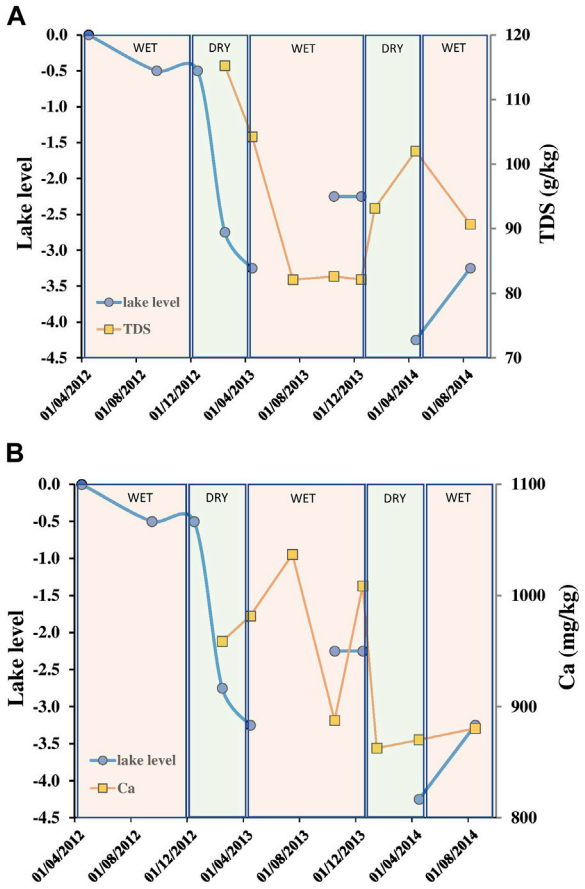

FIGURE 9
(A) Lake level variations and TDS vs. time; **(B)** lake level variations and Ca vs. time.

5.3 REE fractionation induced by mineral dissolution/precipitation

The element loss (Ca*) and element excess (Al*) were calculated to estimate the possible amount of gypsum precipitated and alunite dissolved using the following formula (Table 3):

$$element^{*} = element_{isosol} - element_{analyzed}, \quad (4)$$

where "element $_{isosol}$" is the concentration of the element in the water (ppm) calculated considering the congruent dissolution of the amount of local volcanic rock estimated using the ISOSOL plot, while "element $_{analyzed}$" is the concentration (ppm) of the element analyzed in the lake water. When the element is incorporated in secondary minerals (element loss), element* is a positive value. On the contrary, when the dissolution of secondary minerals occurs (element excess), element* is a negative value. The results show that the loss of Ca, Ca*, varies from 4,268 to 6,757 ppm and the excess of Al, Al*, varies from −1,045 to −2,434 ppm. The values of Ca* and Al* obtained have been used to estimate the amounts of gypsum precipitated and alunite dissolved (Table 3). The results obtained show values of gypsum precipitated up to 29.1 g per liter of lake water, and a maximum of 9.8 g of alunite dissolved per liter of lake water.

As mentioned above, both, gypsum and alunite are capable to incorporate REE during precipitation, especially LREE (Deyell et al., 2005; Inguaggiato et al., 2018; Inguaggiato et al., 2020a; Inguaggiato et al., 2020b; van Hinsberg et al., 2020; Ayora et al., 2021; Pappaterra et al., 2022; Cuadros et al., 2023). To study the effect of gypsum precipitation and alunite dissolution on the chemistry of REE in the waters, REE data in gypsum here presented and REE data in alunite from literature (Deyell et al., 2005) were used to simulate a mass balance calculation. Considering that there are no data in literature about the K_D of REE in alunite and that the concentrations of alunite used for the

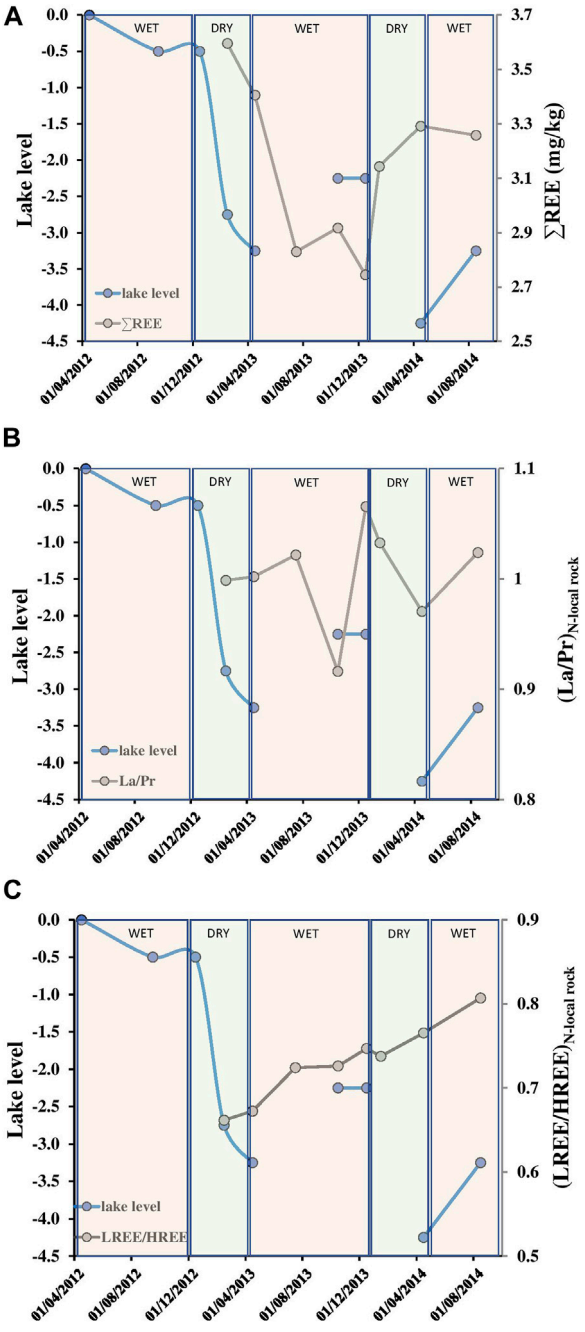

FIGURE 10
(A) Lake level variations and ∑REE vs. time; **(B)** lake level variations and $(La/Pr)_{N\text{-local rock}}$ vs. time; **(C)** lake level variations and $(LREE/HREE)_{N\text{-local rock}}$ vs. time.

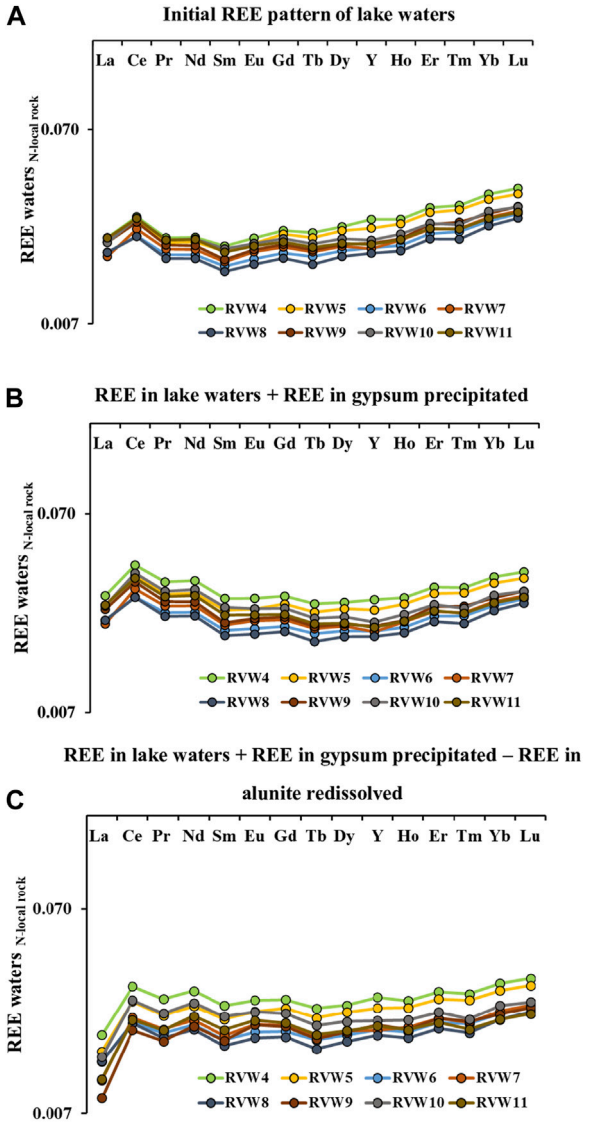

FIGURE 11
(A) Initial REE patterns of lake waters normalized to the average volcanic local rock; **(B)** REE patterns of lake waters after adding the REE concentrations in the amount of gypsum precipitated calculated using the values of Ca loss (Ca*) estimated with the ISOSOL plots; **(C)** REE final patterns of lake waters after adding REE in the gypsum precipitated and subtracting the REE in the grams of alunite dissolved in the lake water calculated using the values of Al excess (Al*) estimated with the ISOSOL plots.

calculation are associated to a different environment (Tambo high-sulfidation deposit, El Indio Pascua belt, Chile; Deyell et al., 2005), the mass balance calculation performed is indicative, giving an idea about the processes ruling the REE relative proportions between each other and it is not necessary representative of the final REE concentrations. The mass balance calculation was performed to estimate the effect of gypsum precipitation and alunite dissolution on the initial LREE depleted patterns in the lake waters (Figure 11A). The complete procedure with all the equations used for the calculation is listed in the Supplementary Material S1.

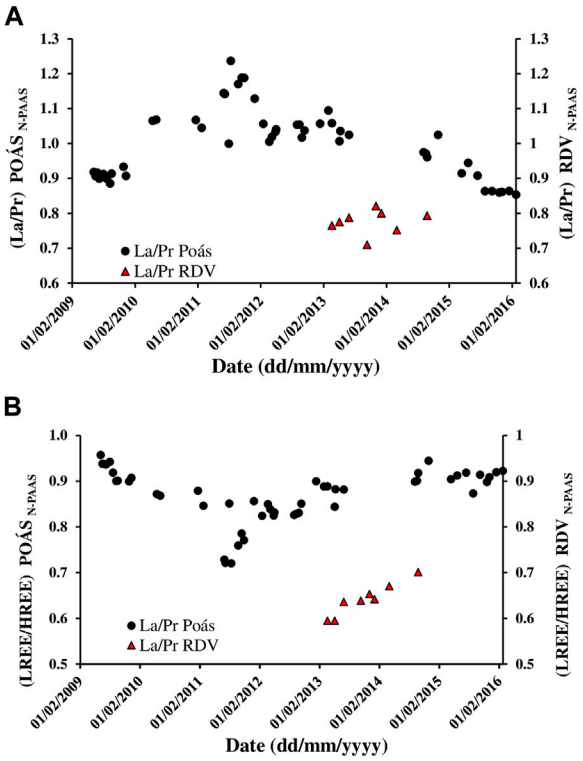

FIGURE 12
(A) $(La/Pr)_{N\text{-}PAAS}$ variations at Poás and Rincón de la Vieja (RDV) crater lakes over time; **(B)** $(LREE/HREE)_{N\text{-}PAAS}$ variations at Poás and Rincón de la Vieja (RDV) crater lakes over time.

The concentrations of REE in gypsum were calculated using the average values of REE K_D and the REE concentration in waters (Table 2). The REE in gypsum calculated were used to estimate the REE concentration for the amount of gypsum precipitated in each sample, estimated with the ISOSOL plot (up to 29.1 g per kg of water; Table 3). The concentration of REE in gypsum estimated for each sample represents the REE concentration supposedly subtracted from the initial water composition by gypsum precipitation and was thus re-added to the initial REE concentrations measured in the lake water. The new patterns of REE normalized to the average local rock show a concavity (Figure 11B), allowing to affirm that the gypsum precipitation process is not enough to track back at the initial point, i.e., to the congruent dissolution of the average local rock, graphically represented by a flat REE pattern. The amount of REE in the alunite redissolved estimated using the ISOSOL plot (up to 9.8 g per kg of water; Table 3) was calculated using data of REE in alunite from Deyell et al. (2005). The results show that only after adding the REE incorporated from the gypsum precipitated and to subtract the REE derived from the alunite dissolution to the REE analyzed in the lake water, the REE pattern normalized to the average local rock is mostly flat (except for La that is depleted respect to the other REE; Figure 11C). The flat REE patterns normalized to the average local rock (Figure 11C) are associated with lake water whose chemistry only reflects the congruent dissolution of the volcanic rocks, and thus the conditions of the water before the precipitation of gypsum and the dissolution of alunite.

5.4 Comparison of REE variations at Poás and Rincón de la Vieja cráter lakes over time

The interest in the chemistry of REE in active volcanic hydrothermal systems over time and their relations with the changes in volcanic activity has increased since the last 2 decades (Takano et al., 2004; Wood, 2006; Morton-Bermea et al., 2010; Varekamp, 2015; Pappaterra et al., 2022).

In the active crater lake of Poás volcano (Costa Rica) REE concentrations were found to vary over time following the main changes in phreatic activity (Pappaterra et al., 2022). In particular, a clear relation exists between the changes of $(La/Pr)_{N\text{-}local\ rock}$ and $(LREE/HREE)_{N\text{-}local\ rock}$ ratios in the Poás crater lake water and the changes in phreatic activity during the period 2009-2016, when more than 700 phreatic eruptions occurred. At Poás crater lake, $(La/Pr)_{N\text{-}local\ rock}$ peaks during a stage of intense phreatic activity (2010–2011) and drops during a period of relative quiescence (2015 - mid-2016). The behavior of $(LREE/HREE)_{N\text{-}local\ rock}$ ratio is opposite with respect to $(La/Pr)_{N\text{-}local\ rock}$ ratio. The relation between the ∑REE, $(La/Pr)_{N\text{-}local\ rock}$ $(LREE/HREE)_{N\text{-}local\ rock}$ ratios and the changes in the phreatic activity is consistent with the correlation between their variations and the changes of the major elements and physico-chemical parameters commonly used for the monitoring of volcanic lakes. $(La/Pr)_{N\text{-}local\ rock}$ ratio shows a positive correlation with all the major elements, some major elements ratios and physico-chemical parameters, except for Ca, that is the only major element that shows a different behavior. Calcium concentrations in the Laguna Caliente water decrease when the intensity of phreatic activity increases, during 2010–2011, similarly to $(LREE/HREE)_{N\text{-}local\ rock}$ ratio (Pappaterra et al., 2022). This different behavior of Ca is consistent with the precipitation of gypsum/anhydrite during that period, making anhydrite/gypsum precipitation a proxy of mineral sealing prior to phreatic eruptions.

In Figure 12 the variations of $(La/Pr)_{N\text{-}PAAS}$ and $(LREE/HREE)_{N\text{-}PAAS}$ ratios during 2009–2016 of Poás crater lake were compared with the variations of the same REE ratios at Rincón de la Vieja crater lake during 2013–2014. The comparison shows that the range of variation of $(La/Pr)_{N\text{-}PAAS}$ and $(LREE/HREE)_{N\text{-}PAAS}$ ratios is higher at Laguna Caliente (0.93–1.35 and 0.71 to 0.95, respectively) than at Rincón de la Vieja crater lake (0.92–1.07 and 0.66 to 0.81, respectively). The diversity in the variation of REE ratios is probably due to the important differences in the state of activity of the two volcanoes during the periods of observation. The intense phreatic activity at Poás volcano induced major variations in the chemistry of the lake (major elements, physico-chemical parameters and REE). Rincón de la Vieja crater lake, instead, passed a period of quiescence, prior to the more intense phreatic activity in more recent years. The small variability of $(La/Pr)_{N\text{-}local\ rock}$ and $(LREE/HREE)_{N\text{-}local\ rock}$ ratios at Rincón de la Vieja crater lake during 2013–2014 is comparable to the variations registered at Poás crater lake during period of low phreatic activity.

6 Conclusion

The major, minor and REE variations at the hyperacid crater lake of Rincón de la Vieja volcano (Costa Rica) have been here investigated during a period of low phreatic activity (2013–2014).

The ∑REE in waters varies over time from 2.7 to 3.6 mg kg^{-1}. The concentrations of REE in waters normalized to the average composition of the local volcanic rocks have LREE depleted patterns. LREE enriched patterns were found in the solids precipitated in laboratory from four lake water samples.

There are no important changes in the chemistry of REE, $(La/Pr)_{N\text{-}local\ rock}$ and $(LREE/HREE)_{N\text{-}local\ rock}$ ratios, associated with the phreatic eruption occurred in mid-2013.

The ISOSOL plot was used to investigate the main processes responsible for the variation in the chemical composition of the lake over time. A high amount of volcanic local rock was dissolved in the crater lake water (110–160 g kg^{-1}). Most of the major and minor elements lie on or near the dissolution line estimated, besides Ca that is always depleted (Ca loss, Ca*), and Al and Na that are always enriched (Al, Na excess; Al*, Na*). The Ca loss is consistent with gypsum/anhydrite precipitation coherently with the SEM-EDS analysis of the solid phase precipitated in laboratory. The Al and Na excess can be explained by Na-alunite dissolution, a mineral likely previously precipitated at the bottom of the lake, or in the deeper volcanic-hydrothermal system. The values of Ca* and Al* estimated with the ISOSOL plot were used to calculate the amount of gypsum precipitated and alunite dissolved. A mass balance calculation was performed to quantify the amount of REE fractionated from the waters due to gypsum precipitation, and the amount of REE re-added to the water due to alunite dissolution. Based on this approach, the LREE patterns observed in crater lake waters could have been induced considering the amounts of gypsum precipitated and of alunite dissolved.

This study confirms that REE are good tracers of the water-rock interaction processes that induce changes in the chemistry of lake waters at active volcanoes. The lack of a clear relation between the variations of ∑REE, $(La/Pr)_{N\text{-}local\ rock}$ and $(LREE/HREE)_{N\text{-}local\ rock}$ ratios and the usual parameters used for volcanic lakes monitoring, as well as the changes in the phreatic activity, does not disprove the effectiveness of these elements to track the changes in the phreatic activity at active crater lakes. The REE slight variability is rather due to the stability of the phreatic activity of Rincón de la Vieja during 2013–2014. Nevertheless, to confirm if REE in active crater lakes are very sensitive to the volcanic activity changes, further studies on similar systems during period of intense phreatic activity, low phreatic activity and quiescence are required.

Data availability statement

The original contributions presented in the study are included in the article/Supplementary Material, further inquiries can be directed to the corresponding author.

Author contributions

CI and SP formulated the scientific question, designed the study and the scientific approach. CI and SP performed the samples treatment in laboratory and their analysis by ICP-MS. SP wrote the original draft of the manuscript and elaborated the data set. CI edited the first draft of the manuscript. RM-A, CR-U, GG, and DR organised and performed the field sampling. LP, GL, TK, and BS revised and edited a version of the manuscript. LB performed the analysis in laboratory by ICP-OES. BS helped with the statistical analysis of the data set. All authors contributed to the article and approved the submitted version.

Funding

This work was supported by: Centro de Investigación Científica y de Educación Superior de Ensenada, Baja California (CICESE, Mexico), within internal project 644170, SENER-CONAHCYT within the CeMIE-Geo Project (207032 Sener-Conacyt 2013-01), Istituto Nazionale di Geofisica e Vulcanologia (INGV; Italy) within "Progetto ricerca libera WADE". This article is part of the doctoral project thesis of SP (supervised by CI) and the authors thank CONAHCYT for funding the doctoral fellowship of SP (1086975).

Acknowledgments

This article is part of the doctoral project thesis of SP (supervised by CI) and the authors thank CONAHCYT for funding the doctoral fellowship (1086975). Authors are grateful to María Margarita Martínez Rodríguez, for helping during the analytical session to analyze REE, Fe, Al, Sr, Ba by ICP-MS in the "Sistema de Laboratorio Especializado de Ciencias de la Tierra" (SLE-CT) in the Centro de Investigación Científica y de Educación Superior de Ensenada, Baja California (CICESE).

Conflict of interest

The authors declare that the research was conducted in the absence of any commercial or financial relationships that could be construed as a potential conflict of interest.

Publisher's note

All claims expressed in this article are solely those of the authors and do not necessarily represent those of their affiliated organizations, or those of the publisher, the editors and the reviewers. Any product that may be evaluated in this article, or claim that may be made by its manufacturer, is not guaranteed or endorsed by the publisher.

Supplementary material

The Supplementary Material for this article can be found online at: https://www.frontiersin.org/articles/10.3389/feart.2023.1197568/full#supplementary-material

References

Alvarado, G. E., and Cárdenes, G. (2017). "Geology, tectonics, and geomorphology of Costa Rica: A natural history approach," in *Costa Rican ecosystem*. Editor M. Kappelle (Chicago: The University of Chicago Press), 30–63. doi:10.7208/9780226121642-008

Alvarado, G. E. (1985). Consideraciones petrologicas de los estratovolcanes de Costa Rica. *Rev. Geol. Amer. Cent.* 3, 103–128. doi:10.15517/rgac.v0i03.10491

Ayora, C., Carrero, S., Bellés, J., Basallote, M. D., Cánovas, C. R., and Marcías, F. (2021). Partition of rare earth elements between sulfate salts formed by the evaporation of acid mine drainage. *Mine water Environ.* 41, 42–57. doi:10.1007/s10230-021-00803-0

Ayres, G. (2012). *Behaviour of rare earth elements during water-rock interaction and alteration processes in volcanic lake systems*. Master thesis. Utrecht University, 108.

Carr, M. J., Feigenson, M. D., Bolge, L. L., Walker, J. A., and Gazel, E. (2013). RU_CAGeochem, a database and sample repository for central American volcanic rocks at rutgers university. *Earth Chem. Libr.* doi:10.1594/IEDA/100403

Chavarria, L., and Rodríguez, A. (2010). Geothermal reconnaissance of the caribbean flank of the Rincón de la Vieja volcano, Costa Rica. *Proc. World Geotherm. Congr.*

Christenson, B. W., Reyes, A. G., Young, R., Moebis, A., Sherburn, S., Cole-Baker, J., et al. (2010). Cyclic processes and factors leading to phreatic eruption events: insights from the 25 september 2007 eruption through Ruapehu crater lake, New Zealand. *J. Volcanol. Geotherm. Res.* 191, 15–32. doi:10.1016/j.jvolgeores.2010.01.008

Christenson, B. W. (2000). Geochemistry of fluids associated with the 1995–1996 eruption of Mt. Ruapehu, New Zealand: signatures and processes in the magmatic-hydrothermal system. *J. Volcanol. Geotherm. Res.* 97, 1–30. doi:10.1016/S0377-0273(99)00167-5

Cuadros, J., Mavris, C., and Nieto, J. M. (2023). Rare earth element signature modifications induced by differential acid alteration of rocks in the Iberian Pyrite Belt. *Chem. Geol.* 619, 121323. doi:10.1016/j.chemgeo.2023.121323

Delmelle, P., Henley, R. W., Opfergelt, S., and Datienne, M. (2015). "Summit acid crater lake and flank instability in composite volcanoes," in *Volcanic lakes*. Editors D. Rouwet, B. W. Christenson, F. Tassi, and J. Vandemeulebrouck (Heidelberg: Springer), 289–306. doi:10.1007/978-3-642-36833-2_12

Delmelle, P., and Bernard, A. (1994). Geochemistry, mineralogy, and chemical modeling of the acid crater lake of Kawah Ijen volcano, Indonesia. *Geochim. Cosmochim. Acta* 58, 2445–2460. doi:10.1016/0016-7037(94)90023-X

Deocampo, D. M., and Jones, B. F. (2014). "Geochemistry of saline lakes," in *Treatise on geochemistry*. Editors H. D. Holland and K. K. Turekian (Oxford: Elsevier), 437–469.

Deyell, C. L., Rye, R. O., Landis, G. P., and Bissing, T. (2005). Alunite and the role of magmatic fluids in the Tambo high-sulfidation deposit, El Indio–Pascua belt, Chile. *Chem. Geol.* 215, 185–218. doi:10.1016/j.chemgeo.2004.06.038

Dutrizac, J. E. (2017). The behaviour of the rare earth elements during gypsum (CaSO4·2H2O) precipitation. *Hydrometallurgy* 174, 38–46. doi:10.1016/j.hydromet.2017.09.013

Ehya, F., and Mazraei, S. M. (2017). Hydrothermal barite mineralization at chenarvardeh deposit, markazi province, Iran: evidences from REE geochemistry and fluid inclusions. *J. Afr. Earth Sci.* 134, 299–307. doi:10.1016/j.jafrearsci.2016.11.006

Fung, A. Y. (2008). "Geothermal resources development in Costa Rica," in *GEOTHERMAL TRAINING PROGRAMME orkustofnun, grensásvegur 9* (Reykjavík, Iceland: GEOTHERMAL TRAINING PROGRAMME).

Gamazo, P., Bea, S. A., Saaltink, M. W., Carrera, J., and Ayora, C. (2011). Modeling the interaction between evaporation and chemical composition in a natural saline system. *J. Hydrol.* 401, 154–164. doi:10.1016/j.jhydrol.2011.02.018

Giggenbach, W. F., and Soto, R. C. (1992). Isotopic and chemical composition of water and steam discharges from volcanic-magmatic-hydrothermal systems of the Guanacaste Geothermal Province, Costa Rica. *App. Geochem.* 7, 309–332. doi:10.1016/0883-2927(92)90022-U

González, G., Fujita, E., Shibazaki, B., Hayashida, T., Chiodini, G., Lucchi, F., et al. (2021). Increment in the volcanic unrest and number of eruptions after the 2012 large earthquakes sequence in Central America. *Sci. Rep.* 11, 22417. doi:10.1038/s41598-021-01725-1

Guichard, F., Chruch, T. M., Treuil, M., and Jaffrezic, H. (1979). Rare earths in barites: distribution and effects on aqueous partitioning. *Geochim. Cosmochim. Acta* 43, 983–997. doi:10.1016/0016-7037(79)90088-7

Henley, R. W., and Ellis, A. J. (1983). Geothermal systems ancient and modern: A geochemical review. *Earth Sci. Rev.* 19, 1–50. doi:10.1016/0012-8252(83)90075-2

Inguaggiato, C., Burbano, V., Rouwet, D., and Garzon, G. (2017). Geochemical processes assessed by rare earth elements fractionation at "Laguna Verde" acidic-sulphate crater lake (Azufral volcano, Colombia). *Appl. Geochem.* 79, 65–74. doi:10.1016/j.apgeochem.2017.02.013

Inguaggiato, C., Censi, P., Zuddas, P., Londono, J. M., Chacon, Z., Alzate, D., et al. (2015). Geochemistry of REE, Zr and Hf in a wide range of pH and water composition: the Nevado del Ruiz volcano-hydrothermal system (Colombia). *Chem. Geol.* 417, 125–133. doi:10.1016/j.chemgeo.2015.09.025

Inguaggiato, C., Iñiguez, E., Peiffer, L., Kretzschmar, T., Brusca, L., Mora-Amador, R., et al. (2018). REE fractionation during the gypsum crystallization in hyperacid sulphate-rich brine: the Poás volcano crater lake (Costa Rica) exploited as laboratory. *Gondwana Res.* 59, 87–96. doi:10.1016/j.gr.2018.02.022

Inguaggiato, C., Pappaterra, S., Peiffer, L., Apollaro, C., Brusca, L., De Rosa, R., et al. (2020a). Mobility of REE from a hyperacid brine to secondary minerals precipitated in a volcanic hydrothermal system: kawah Ijen crater lake (java, Indonesia). *Sci. Total Environ.* 740, 1–14. doi:10.1016/j.scitotenv.2020.140133

Inguaggiato, C., Pérez García, M. A., Meza Maldonado, L. F., Peiffer, L., Pappaterra, S., and Brusca, L. (2020b). Precipitation of secondary minerals in acid sulphate-chloride waters traced by major, minor and rare earth elements in waters: the case of puracé volcano (Colombia). *J. Volcanol. Geotherm. Res.* 408, 107106–107110. doi:10.1016/j.jvolgeores.2020.107106

Instituto Meteorológico Nacional (INM) (2022). Boletín meteorológico mensual. Avaliable At: https://www.imn.ac.cr.

Kempter, K. A., Benner, S. G., and Williams, S. N. (1996). Rincón de la Vieja volcano, Guanacaste province, Costa Rica: geology of the southwestern flank and hazards implications. *J. Volcanol. Geotherm. Res.* 71, 109–127. doi:10.1016/0377-0273(95)00072-0

Kempter, K. A., and Rower, G. L. (2000). Leakage of Active Crater lake brine through the north flank at Rincón de la Vieja volcano, northwest Costa Rica, and implications for crater collapse. *J. Volcanol. Geotherm. Res.* 97, 143–159. doi:10.1016/S0377-0273(99)00181-X

Komor, S. C. (1992). Bidirectional sulfate diffusion in saline-lake sediments: evidence from devils lake, northeast north Dakota. *Geology* 20, 319–322. doi:10.1130/0091-7613(1992)020<0319:BSDISL>2.3.CO;2

Komor, S. C. (1994). "Bottom-sediment chemistry in devils lake, northeast north Dakota," in *Sedimentology and geochemistry of modern and ancient saline lakes*. Editors R. W. Renaut and W. M. Last (Society for Sedimentary Geology) Special Publication), 21–32. doi:10.2110/pec.94.50.0021

Lin, J., Nilges, M. J., Wiens, E., Chen, N., Wang, S., and Pan, Y. (2019). Mechanism of Gd3+ uptake in gypsum (CaSO4·2H2O): implications for EPR dating, REE recovery and REE behavior. *Geochim. Cosmochim. Acta* 258, 63–78. doi:10.1016/j.gca.2019.05.019

Martínez, M. (2008). *Geochemical evolution of the acidic crater lake of Poás volcano (Costa Rica): Insight into volcanic-hydrothermal processes*. Ph.D., Thesis. Universiteit Utrecht: IAVCEI, 162p.

Miller, J. L., Elwood Madden, M. E., Elwood Madden, A. S., and Princhett, B. N. (2014). Temperature, pH and brine effect on alunite dissolution: implications for mars. *45th Lunar Planet. Sci. Conf.*

Morton-Bermea, O., Armienta, M. A., and Ramos, S. (2010). Rare-earth element distribution in water from El Chichón volcano crater lake, chiapas Mexico. *Geofísica Int.* 49 (1), 43–54. doi:10.22201/igeof.00167169p.2010.49.1.1474

Observatorio Vulcanológico y Sismológico de Costa Rica, OVSICORI (2022). Open reports. Avaliable At: http://www.ovsicori.una.ac.cr.

Pappaterra, S., Inguaggiato, C., Rouwet, D., Mora-Amador, R., Ramírez-Umaña, C., González, G., et al. (2022). Rare earth elements variations in a hyperacid crater lake and their relations with changes in phreatic activity, physico-chemical parameters, and chemical composition: the case of Poás volcano (Costa Rica). *Front. Earth Sci.* 9, 138–159. doi:10.3389/feart.2021.716970

Red Sismológica Nacional, Universidad de Costa Rica, RSN:UCR-ICE (2023). Reportes volcanicos. Avaliable At: https://rsn.ucr.ac.cr.

Rodríguez, A., van Bergen, M. J., and Eggenkamp, H. G. M. (2018). Experimental evaporation of hyperacid brines: effects on chemical composition and chlorine isotope fractionation. *Geochim. Cosmochim. Acta* 222, 467–484. doi:10.1016/j.gca.2017.10.032

Rodríguez, A., and van Bergen, M. J. (2017). Superficial alteration mineralogy in active volcanic systems: an example of Poás volcano, Costa Rica. *J. Volcanol. Geotherm. Res.* 346, 54–80. doi:10.1016/j.jvolgeores.2017.04.006

Rouwet, D., Mora Amador, R. A., Sandri, L., Ramírez-Umaña, C., González, G., Pecoraino, G., et al. (2019). "39 years of geochemical monitoring of Laguna Caliente crater lake, Poás: patterns from the past as key for the future," in *Poás volcano (Costa Rica): The pulsing heart of Central America volcanic zone*. Editors F. Tassi, R. Mora-Amador, and O. Vaselli (Heidelberg: Springer), 231–234. doi:10.1007/978-3-319-02156-0_9

Rouwet, D., Mora-Amador, R., Ramirez-Umana, C. J., Gonzalez, G., and Inguaggiato, S. (2017). "Dynamic fluid recycling at Laguna Caliente (Poás, Costa Rica) before and during the 2006–ongoing phreatic eruption cycle (2005–10)," in *Geochemistry and geophysics of active volcanic lakes, special publications*. Editors T. Ohba, B. Capaccioni, and C. Caudron (Geological Society of London), 73–96. doi:10.1144/SP437.11

Rouwet, D., Tassi, F., Mora-Amador, R., Sandri, L., and Chiarini, V. (2014). Past, present and future of volcanic lake monitoring. *J. Volcanol. Geotherm. Res.* 272, 78–97. doi:10.1016/j.jvolgeores.2013.12.009

Rowe, G. L., Ohsawa, S., Takano, B., Brantley, S. L., Fernández, J. F., and Barquero, J. (1992). Using Crater lake chemistry to predict volcanic activity at Poás volcano, Costa Rica. *Bull. Volcanol.* 54, 494–503. doi:10.1007/BF00301395

Shannon, R. D., and Prewitt, C. T. (1969). Effective ionic radii in oxides and fluorides. *Acta Cryst. B* 25, 925–946. doi:10.1107/S0567740869003220

Smithsonian Institute and Global Volcanism Program (2023). Open reports. Avaliable At: https://volcano.si.edu.

Soto, G., Alvarado, G. E., and Goold, S. (2004). Erupciones < 3800 A.P. del volcán Rincón de la Vieja, Costa Rica. *Rev. Geol. América Cent.* 29, 67–86. doi:10.15517/rgac.v0i29.7776

Takano, B., Suzuki, K., Sugimori, K., Ohba, T., Fazlullin, S. M., Bernard, A., et al. (2004). Bathymetric and geochemical investigation of kawah Ijen crater lake, east java, Indonesia. *J. Volcanol. Geotherm. Res.* 135, 299–329. doi:10.1016/j.jvolgeores.2004.03.008

Tassi, F., Vaselli, O., Bini, G., Capecchiacci, F., de Moor, J. M., Pecoraino, G., et al. (2018). The geothermal resource in the Guanacaste region (Costa Rica): new hints from the geochemistry of naturally discharging fluids. *Front. Earth Sci.* 6, 69. doi:10.3389/feart.2018.00069

Tassi, F., Vaselli, O., Capaccioni, B., Giolito, C., Duarte, E., Fernandez, E., et al. (2005). The hydrothermal-volcanic system of Rincon de la Vieja volcano (Costa Rica): A combined (inorganic and organic) geochemical approach to understanding the origin of the fluid discharges and its possible application to volcanic surveillance. *J. Volcanol. Goetherm. Res.* 148, 315–333. doi:10.1016/j.jvolgeores.2005.05.001

Tassi, F., Vaselli, O., Fernandez, E., Duarte, E., Martínez, M., Delgado Huertas, A., et al. (2009). Morphological and geochemical features of crater lakes in Costa Rica: an overview. *J. Limnol.* 68 (2), 193–205. doi:10.4081/jlimnol.2009.193

Toner, J. D., Catling, D. C., and Light, B. (2015). Modeling salt precipitation from brines on mars: evaporation versus freezing origin for soil salts. *Icarus* 250, 451–461. doi:10.1016/j.icarus.2014.12.013

Van Hinsberg, V., Berlo, K., and Lowenstern, J. (2020). An experimental investigation of interaction between andesite and hyperacidic volcanic lake water. *Minerals* 10, 96–21. doi:10.3390/min10020096

van Hinsberg, V., Vigouroux, N., Palmer, S., Berlo, K., Mauri, G., Williams-Jones, A., et al. (2017). Element flux to the environment of the passively degassing crater lake-hosting Kawah Ijen volcano, Indonesia, and implications for estimates of the global volcanic flux. *Geol. Soc.* 437 (1), 9–34. doi:10.1144/SP437.2

Varekamp, J. C., Ouimette, A. P., Herman, S. W., Flynn, K. S., Bermudez, A., and Delpino, D. (2009). Naturally acid waters from Copahue volcano, Argentina. *Appl. Geochem.* 24 (2), 208–220. doi:10.1016/j.apgeochem.2008.11.018

Varekamp, J. C., Pasternack, G. B., and Rowe, G. L. (2000). Volcanic lake systematics. II. chemical constraints. *J. Volcanol. Geotherm. Res.* 97, 161–179. doi:10.1016/S0377-0273(99)00182-1

Varekamp, J. C. (2015). "The chemical composition and evolution of volcanic lakes," in *Volcanic lakes*. Editors D. Rouwet, B. W. Christenson, F. Tassi, and J. Vandemeulebrouck (Heidelberg: Springer), 93–123. doi:10.1007/978-3-642-36833-2_

Wood, S. A. (2006). Rare earth element systematics of acidic geothermal waters from the Taupo Volcanic Zone, New Zealand. *J. Geochem. Explor.* 89, 424–427. doi:10.1016/j.gexplo.2005.11.023